Journal of Optimization Theory and Applications (2023) 198:988–1018
https://doi.org/10.1007/s10957-023-02278-1

The Game of Two Identical Cars: An Analytical Description of the Barrier

Maksim Buzikov[1] · **Andrey Galyaev**[1]

Received: 7 July 2022 / Accepted: 14 July 2023 / Published online: 31 July 2023

Abstract

In this study, a pursuit-evasion game of two players, known as a game of two identical cars, is examined. It is assumed that the game proceeds in a two-dimensional plane. Both players have a constant speed and a limited turn radius. The goal of the first player (pursuer) is to ensure that the second player (evader) enters the capture circle as quickly as possible. The goal of the evader is to avoid or delay capturing for as long as possible. The kinematics of both players are described using the same equations. Thus, the game has only one free parameter: capture radius. This study aims to provide an exhaustive analytical description of the barrier surface for all values of capture radius. Previously, Merz analytically investigated the barrier in a game of two identical cars. In this work, it was found that there is a certain critical value of the capture radius, above which the barrier is qualitatively different from Merz's example. In addition, we obtained an explicit analytical description of the optimal feedback controls for the barrier.

Keywords Game of two cars · Non-holonomic constraints · Differential Game · Min–max strategies · Barriers

Mathematics Subject Classification 49N90 · 49N75

Communicated by Mauro Pontani.

✉ Maksim Buzikov
me.buzikov@physics.msu.ru

Andrey Galyaev
galaev@ipu.ru

[1] V. A. Trapeznikov Institute of Control Sciences of Russian Academy of Sciences, Moscow, Russia

1 Introduction

The game of two cars (GTC) was originally described and investigated by Isaacs in the 1950s. In his seminal work [9, pp. 237–244], Isaacs obtained a partial description of the barrier for this problem and a description of the singular lines on the barrier. Isaacs supposed that the independent parameters of the problem (capture radius, speed ratio, and minimum turn radius ratio) are such that capture is possible from an arbitrary initial state. Thus, the barrier explored by Isaacs was not closed. In [6], Cockayne revealed necessary and sufficient conditions for the parameters of the interception problem from an arbitrary initial state. These conditions were refined by Rublein in [30]. The necessary and sufficient conditions for the existence of an evasion strategy are presented in [3]. Publications [3, 6, 30] assume that interception is the coincidence of pursuer and evader planar coordinates. This corresponds to the zero-capture radius. In [9, 19], Isaacs and Merz intensively investigated the case of a GTC with a zero minimum turn radius for the evader (the homicidal chauffeur game). A complete analysis and modern discussion of this case are provided in [27]. In [4], Breakwell and Merz calculated the minimal capture radius, which always permits interception from an arbitrary initial state for a given speed ratio and a minimum turn radius ratio. A new criterion for full state-space capturability based on the barrier geometry was proposed in [28]. If the origin of the coordinate system is bonded with the pursuer (the y-axis is aligned with the velocity of the pursuer) and the barrier surface does not cross the positive y-axis, then the pursuer can intercept the evader from any initial state. Later, Pachter and Miloh revealed new regions of the parameter space in which the open barrier surface qualitatively differs from previously observed types [29]. An optimal feedback control synthesis for GTC was introduced in [32, 34] by Simakova. Simakova investigated the value of the game in [35] and the game of kind in [33]. Her results are applicable only in a special case when the pursuer surpasses all parameters of the evader. In addition, she considers only a state-space region, where the value of the game is a smooth function. In [10], Simakova examined the obtained results in comparison with other methods such as proportional navigation. In [7], Farber and Shinar described a methodology to obtain an approximate solution and compared it with Simakova's solution. A computational approach based on discretization of the GTC was presented in [1, pp. 48–60]. In [2], Bera et al. investigated and visualized singular surfaces of the game in a wide range of parameters. A comprehensive survey of GTC in the context of pursuit-evasion differential games was presented in [43].

The solution of the GTC can be utilized for a collision avoidance problem, where it is supposed that there is no cooperation between the players, and the evader has to imply a strategy such that its use will lead to escape for any strategy of the pursuer. It is assumed that the evader is a plant and the pursuer plays the role of a moving obstacle. The formal problem statement remains the same. Usually, the parameters of the collision avoidance problem differ from those of a pursuit-evasion problem in that the pursuer does not have the advantage of speed and minimum turn radius. In [16], Meier introduced a method for obtaining the capture region when it is bounded. His method was based on an analysis of reachable sets. Initially, the reachable sets of pursuer and evader at a given time were determined. Furthermore, by combining these loci for various fixed times and a fixed initial state, the capture region can

be determined by finding envelopes and intersections. In [5, 18, 20], Merz et al. examined a cooperative collision avoidance problem with equations of motion of the GTC. Cooperative collision avoidance implies the maximization of the distance to the closest point of approach by both players instead of maximizing the time to collision by the evader in the pursuit-evasion game. Further, Miloh and Sharma supplemented Merz's results and investigated the barrier surface for a collision avoidance problem for cooperative maneuvers of players [21, 31]. In [40, 41], Vincent et al. analyzed the problem of collision avoidance of two vehicles when there is no cooperation among players. The main idea of the analysis is to divide the state space into vulnerability zones. The "red" zone corresponds to a win region of the pursuer in the GTC. Therefore, the boundary of the red zone is a barrier surface for the GTC. In [40], an analytical description of the barrier in the case of an evader's superiority in terms of parameters was provided. In [42], the same authors supplemented their analysis by considering a proportional navigation strategy for the pursuer. Papers [22, 26] examined a collision avoidance problem for line segments and elliptical players. In [23, 24], an extended kinematic model that considers the variable speeds of players was examined. In [11], Kwik calculated the escape maneuver for the evader if the pursuer maneuver was known.

A game of two identical cars (GTIC) was originally considered by Merz in [17]. In GTIC, it is assumed that the speeds and minimum-turn radii of the players are the same. After choosing an appropriate description of the GTIC statement, there is only one parameter in the problem: capture radius. In [17], Merz described the barrier of the game, the universal, and dispersal surfaces. A game of surveillance-evasion of two identical cars is considered by Greenfeld in [8]. The difference from GTIC is that the game set is inside the capture circle. Moreover, the pursuer maximizes, whereas the evader minimizes the escape time. In [25], Mitchell used the description of the barrier obtained by Merz to validate a solver of the Hamilton-Jacobi equation. A cooperative collision avoidance problem of two identical cars is completely analyzed by Tarnopolskaya and Fulton in [36]. Furthermore, these authors examined more general cases of unequal parameters of players in [13–15, 37–39].

Although the GTIC has been intensively studied, there are some unexplored questions regarding this problem. The analytical description of the barrier presented in [17, 25] is constrained only by the parametric equations of the surfaces that constitute the barrier. These publications do not provide analytical conditions for the limitations of the parameter domains in the description of surfaces, that is, there are no conditions for cutting off excess parts of these surfaces. The same can be said about the description of universal and dispersal surfaces from [17]. In addition, Merz noted an unexpected result in the numerical calculation of the angular slice of the dispersal surface at a sufficiently small angle between the velocities of the players. Analytical analysis of this phenomenon is not covered in the available sources.

This paper is devoted to a complete analytical description of the barrier surface. The analysis shows that for different values of the capture radius, there is a different analytical description of the conditions for cutting off the excess parts of the surfaces that form the barrier. Instead of using the trial-and-error approach from [25], we present a systematic method for constructing the barrier surface. This study also proposes efficient methods for calculating the optimal feedback controls for players and provides

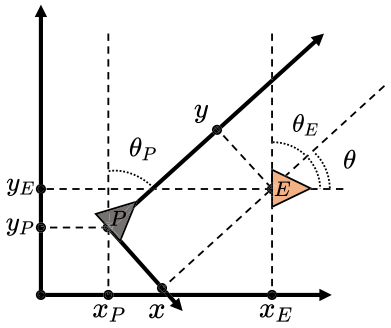

Fig. 1 Players in the realistic space $\begin{bmatrix} x_P & y_P & \theta_P & x_E & y_E & \theta_E \end{bmatrix}^\top$ and reduced space $\begin{bmatrix} x & y & \theta \end{bmatrix}^\top$

an explicit analytical expression for the barrier surface parameterization in terms of the state vector.

The remainder of this paper is organized as follows. Section 2 provides a mathematical description of GTIC. Section 3 describes the strategies of players in terms of the state and adjoint vectors. Section 4 is devoted to an analytical description of the barrier and its form depending on the capture radius. Section 5 provides a synthesis of optimal feedback controls for players and proposes an explicit analytical description of the barrier in terms of the state vector. Finally, Sect. 6 presents conclusions.

2 Problem Formulation

In this section, we formulate a mathematical statement for the GTIC. We use the notation $\boldsymbol{z} = \begin{bmatrix} x & y & \theta \end{bmatrix}^\top \in \mathbb{R}^2 \times \mathbb{S}$ for a configuration, which is a planar position and orientation triplet. Throughout this paper, the subscripts P and E refer to pursuer and evader configurations, respectively (Fig. 1).

For the GTIC, the kinematics of each player is described using the Dubins model. According to this model, the pursuer and evader configurations in a realistic space can be written as $\begin{bmatrix} x_P & y_P & \theta_P \end{bmatrix}^\top$ and $\begin{bmatrix} x_E & y_E & \theta_E \end{bmatrix}^\top$, respectively (see Fig. 1). All angles were counted in the clockwise direction along the y-axis. In the reduced space, we associate the coordinate system with the pursuer position and align the y-axis with the velocity of the pursuer. The equations of motion of the GTIC [17, Eq. 2] are presented as

$$\dot{\boldsymbol{z}} = \begin{bmatrix} \dot{x} \\ \dot{y} \\ \dot{\theta} \end{bmatrix} = \begin{bmatrix} -uy + \sin\theta \\ -1 + ux + \cos\theta \\ v - u \end{bmatrix} \stackrel{\text{def}}{=} \boldsymbol{f}(\boldsymbol{z}, \boldsymbol{u}, \boldsymbol{v}). \tag{1}$$

Here, the pursuer and evader controls correspond to functions

$$u(\boldsymbol{z}) \stackrel{\text{def}}{=} \boldsymbol{u}(\boldsymbol{z}) \in \mathcal{U} \stackrel{\text{def}}{=} [-1, +1], \quad v(\boldsymbol{z}) \stackrel{\text{def}}{=} \boldsymbol{v}(\boldsymbol{z}) \in \mathcal{V} \stackrel{\text{def}}{=} [-1, +1],$$

where $\mathcal{U}$ and $\mathcal{V}$ are the constrained ranges of players' controls.

The set of all possible states defined as the game set is given by

$$\mathcal{S} \stackrel{\text{def}}{=} \{z \in \mathbb{R}^2 \times \mathbb{S} : \ x^2 + y^2 \geq \ell^2\},$$

where $\ell \in \mathbb{R}^+$ is the capture radius of the target set $\mathcal{C} = \partial\mathcal{S}$. We suppose that the game starts from the initial state $z_0 \in \mathcal{S}$ at the time moment $t = 0$, then the current state of the game $z(t) = \left[x(t)\ y(t)\ \theta(t)\right]^\top$ depends on the players' controls and it can be defined as a solution of the equations of motion (1). The game terminates if the state reaches the target set for the first time at $t_f \in \mathbb{R}_0^+$. Further, we associate subscript f with some final states throughout this paper. If the target set cannot be reached for given controls, we assume that $t_f = +\infty$.

The terminal state $z(t_f)$ in the target set can be represented in a more convenient form. Let $s = \left[\varphi_f\ \theta_f\right]^\top \in \mathbb{S}^2$. The target set can be presented as

$$\mathcal{C} = \{z_{\mathcal{C}}(s) : \ s \in \mathbb{S}^2\}, \ \text{where } z_{\mathcal{C}}(s) \stackrel{\text{def}}{=} \left[\ell \sin\varphi_f\ \ell\cos\varphi_f\ \theta_f\right]^\top.$$

The polar angle φ_f fixes the planar position in the capture circle.

The outcome functional of the game is

$$J[\boldsymbol{u}(\cdot), \boldsymbol{v}(\cdot); z_0] \stackrel{\text{def}}{=} \int_0^{t_f} L(z(t), \boldsymbol{u}(z(t)), \boldsymbol{v}(z(t)))\mathrm{d}t + G(z(t_f)),$$

where the running cost function $L(z, \boldsymbol{u}, \boldsymbol{v}) = 1$ and the terminal cost function $G(z) = 0$. The pursuer strives to minimize the outcome functional when the evader maximizes it. For the optimal feedback controls $\boldsymbol{u}^*(\cdot)$, $\boldsymbol{v}^*(\cdot)$ and for any other admissible controls $\boldsymbol{u}(\cdot)$, $\boldsymbol{v}(\cdot)$ the following inequalities hold

$$J[\boldsymbol{u}^*(\cdot), \boldsymbol{v}(\cdot); z_0] \leq V(z_0) \stackrel{\text{def}}{=} J[\boldsymbol{u}^*(\cdot), \boldsymbol{v}^*(\cdot); z_0] \leq J[\boldsymbol{u}(\cdot), \boldsymbol{v}^*(\cdot); z_0].$$

If the pursuer and evader play optimally, the value $V(z_0)$ is the time to capture.

It is obvious that there is a set of states in which the evader can escape with any pursuer strategy. For example, if the velocities of players are collinear ($\theta = 0_{\mathbb{S}}$) and the evader is in front of the pursuer, then control $v(z) = 0$ guarantees evasion. It follows that escape set $\mathcal{F} \subset \mathcal{S}$ is not empty. We denote $\mathcal{W} \subset \mathcal{S}$ as a capture set. The boundary separating the capture set from the escape set is a barrier $\mathcal{B} \subset \mathcal{S}$. In the remainder of this paper, we describe barrier $\mathcal{B}$ analytically. In addition, we provide controls $\boldsymbol{u}^*(z)$ and $\boldsymbol{v}^*(z)$ for $z \in \mathcal{B}$.

3 Main Equation

If the initial state of the game lies on the barrier surface and both players use optimal strategies, then the state vector does not leave the barrier. This means that the evader

must be able to set the value of its control in such a way that it prevents the state vector from penetrating the capture set $\mathcal{W}$ while the pursuer keeps the state out of the escape set $\mathcal{F}$ in the same way. The property described to prevent penetration constitutes the concept of semi-permeability.

Let $\nu_z = \begin{bmatrix}\nu_x & \nu_y & \nu_\theta\end{bmatrix}^\top \in \mathbb{R}^3$ denote a normal vector of barrier $\mathcal{B}$ at some point. The length of ν_z is not necessarily a unit. According to Isaacs [9, pp. 205–210], the condition that $\mathcal{B}$ be a semipermeable surface

$$\min_{\boldsymbol{u}\in\mathcal{U}} \max_{\boldsymbol{v}\in\mathcal{V}} (\nu_z, \boldsymbol{f}(z, \boldsymbol{u}, \boldsymbol{v})) = 0 \tag{2}$$

for all $z \in \mathcal{B}$. In the particular case of the GTIC, the right part of equations of motion is separable and it can be presented in a special form

$$\boldsymbol{f}(z, \boldsymbol{u}, \boldsymbol{v}) = \boldsymbol{f}_P(z, \boldsymbol{u}) + \boldsymbol{f}_E(z, \boldsymbol{v}) + \boldsymbol{g}(z),$$

where we have set

$$\boldsymbol{f}_P(z, \boldsymbol{u}) \stackrel{\text{def}}{=} \begin{bmatrix} -uy \\ ux \\ -u \end{bmatrix}, \quad \boldsymbol{f}_E(z, \boldsymbol{v}) \stackrel{\text{def}}{=} \begin{bmatrix} 0 \\ 0 \\ v \end{bmatrix}, \quad \boldsymbol{g}(z) \stackrel{\text{def}}{=} \begin{bmatrix} \sin\theta \\ -1+\cos\theta \\ 0 \end{bmatrix}.$$

Functions $\boldsymbol{f}_P(\cdot)$ and $\boldsymbol{f}_E(\cdot)$ are linear in the components of the controls for both players. It follows that the main equation (2) can be analyzed by investigating the switch functions [12, pp. 147–148]. We will denote by

$$s_P(z, \nu_z) \stackrel{\text{def}}{=} y\nu_x - x\nu_y + \nu_\theta, \quad s_E(z, \nu_z) \stackrel{\text{def}}{=} \nu_\theta$$

the switch functions of the pursuer and evader. The main equation (2) helps to determine candidates to player optimal control depending on the state z and normal vector ν_z

$$\tilde{u}(z, \nu_z) \stackrel{\text{def}}{=} \arg\min_{\boldsymbol{u}\in\mathcal{U}} (\nu_z, \boldsymbol{f}_P(z, \boldsymbol{u})), \quad \tilde{v}(z, \nu_z) \stackrel{\text{def}}{=} \arg\max_{\boldsymbol{v}\in\mathcal{V}} (\nu_z, \boldsymbol{f}_E(z, \boldsymbol{v})). \tag{3}$$

Applying the notions of switch functions we obtain

$$(\boldsymbol{\nu}_z, \boldsymbol{f}_P(z, \boldsymbol{u})) = -us_P(z, \nu_z), \quad (\boldsymbol{\nu}_z, \boldsymbol{f}_E(z, \boldsymbol{v})) = vs_E(z, \nu_z). \tag{4}$$

The construction of semipermeable surface uses the evolution of normal vector ν_z [12, pp. 113–114] described by the adjoint equations

$$\dot{\nu}_z \stackrel{\text{def}}{=} \begin{bmatrix} \dot{\nu}_x \\ \dot{\nu}_y \\ \dot{\nu}_\theta \end{bmatrix} = -\frac{\partial \boldsymbol{f}(z, \boldsymbol{u}, \boldsymbol{v})}{\partial z}\nu_z = \begin{bmatrix} -u\nu_y \\ u\nu_x \\ -\nu_x\cos\theta + \nu_y\sin\theta \end{bmatrix}. \tag{5}$$

These equations hold along the barrier paths. Let $\nu_z(t) = \left[\nu_x(t)\ \nu_y(t)\ \nu_\theta(t)\right]^\top$ denote a solution of this system at the time moment t.

Lemma 3.1 *In GTIC, the candidate optimal control laws $\tilde{u}(\cdot)$ and $\tilde{v}(\cdot)$ are given by*

$$\tilde{u}(z,\nu_z) = \begin{cases} \operatorname{sgn} s_P(z,\nu_z), & s_P(z,\nu_z) \neq 0; \\ \operatorname{sgn} \nu_x, & s_P(z,\nu_z) = 0,\ \nu_x \neq 0; \\ 0, & s_P(z,\nu_z) = 0,\ \nu_x = 0,\ \nu_y < 0; \\ u \in \{-1,0,+1\}, & \text{otherwise}, \end{cases}$$

$$\tilde{v}(z,\nu_z) = \begin{cases} \operatorname{sgn} s_E(z,\nu_z), & s_E(z,\nu_z) \neq 0; \\ \operatorname{sgn}(\nu_x\cos\theta - \nu_y\sin\theta), & s_E(z,\nu_z) = 0,\ \nu_y\sin\theta \neq \nu_x\cos\theta; \\ 0, & s_E(z,\nu_z) = 0,\ \nu_y\sin\theta = \nu_x\cos\theta,\ \nu_x\sin\theta < -\nu_y\cos\theta; \\ v \in \{-1,0,+1\}, & \text{otherwise}. \end{cases}$$

Proof These expressions were obtained from [17]. □

In the remainder of this section, we provide solutions to (1) and (5) for fixed values u and v of the controls [17, 25]. These solutions are required to investigate the barrier emanation in the next section. It is more convenient to explore emanation by using the retrograde time variable $\tau = t_f - t$. Let $\tilde{z} = \left[\tilde{x}\ \tilde{y}\ \tilde{\theta}\right]^\top \in \mathbb{R}^2 \times \mathbb{S}$. The integration of (1) using the fixed values of controls $u \in \mathcal{U}$, $v \in \mathcal{V}$ and the condition $z(t_f) = \tilde{z}$ leads to the following solution:

$$\begin{aligned} z_{u,v}(\tau;\tilde{z}) &\stackrel{\text{def}}{=} z(t_f - \tau) \\ &= \begin{bmatrix} \tilde{x}\cos u\tau + \tilde{y}\sin u\tau + \frac{u\tau^2}{2}\operatorname{sinc}^2\frac{u\tau}{2} - \tau\operatorname{sinc}\frac{v\tau}{2}\sin\left(\tilde{\theta} + \left(u - \frac{v}{2}\right)\tau\right) \\ \tilde{y}\cos u\tau - \tilde{x}\sin u\tau + \tau\operatorname{sinc}\frac{u\tau}{2} - \tau\operatorname{sinc}\frac{v\tau}{2}\cos\left(\tilde{\theta} + \left(u - \frac{v}{2}\right)\tau\right) \\ \tilde{\theta} + (u - v)\tau \end{bmatrix}. \end{aligned} \tag{6}$$

The distance between players on the plane is equal to

$$r_{u,v}(\tau;\tilde{z}) \stackrel{\text{def}}{=} \sqrt{(z_{u,v}(\tau;\tilde{z}), \boldsymbol{I}_{XY} z_{u,v}(\tau;\tilde{z}))},\ \text{where}\ \boldsymbol{I}_{XY} \stackrel{\text{def}}{=} \begin{bmatrix} 1 & 0 & 0 \\ 0 & 1 & 0 \\ 0 & 0 & 0 \end{bmatrix}. \tag{7}$$

Let $\tilde{\nu}_z = \left[\tilde{\nu}_x\ \tilde{\nu}_y\ \tilde{\nu}_\theta\right]^\top \in \mathbb{R}^3$ and $\nu_z(t_f) = \tilde{\nu}_z$. In turn, integrating (5) leads to

$$\nu_z^{u,v}(\tau;\tilde{z},\tilde{\nu}_z) \stackrel{\text{def}}{=} \nu_z(t_f - \tau) = \begin{bmatrix} \tilde{\nu}_x\cos u\tau + \tilde{\nu}_y\sin u\tau \\ \tilde{\nu}_y\cos u\tau - \tilde{\nu}_x\sin u\tau \\ \tilde{\nu}_\theta + \tau\operatorname{sinc}\frac{v\tau}{2}\left(\tilde{\nu}_x\cos\left(\tilde{\theta} - \frac{v\tau}{2}\right) - \tilde{\nu}_y\sin\left(\tilde{\theta} - \frac{v\tau}{2}\right)\right) \end{bmatrix}.$$

This solution also requires the controls to have fixed values.

4 Barrier

The first step in barrier construction is to determine the usable part ($\mathcal{UP}$) and its boundary. By definition, the usable part is the part of the target set where the pursuer can guarantee termination regardless of the choice of control by the evader [12, pp. 39–40]. The unit normal of the target set $\mathcal{C}$ directed into the game set $\mathcal{S}$ at some point $\boldsymbol{z}_{\mathcal{C}}(\boldsymbol{s})$ for $\boldsymbol{s} \in \mathbb{S}^2$ will be denoted by $\boldsymbol{n}_{\mathcal{C}}(\boldsymbol{s}) = \begin{bmatrix}\sin\varphi_f & \cos\varphi_f & 0\end{bmatrix}^\top \in \mathbb{R}^3$. The pursuer can guarantee the termination when the velocity vector penetrates the target set. Hence,

$$\begin{aligned}\mathcal{UP} &\stackrel{\text{def}}{=} \left\{\boldsymbol{z}_{\mathcal{C}}(\boldsymbol{s}) : \boldsymbol{s} \in \mathbb{S}^2,\ \min_{\boldsymbol{u}\in\mathcal{U}}\max_{\boldsymbol{v}\in\mathcal{V}}(\boldsymbol{n}_{\mathcal{C}}(\boldsymbol{s}),\ \boldsymbol{f}(\boldsymbol{z}_{\mathcal{C}}(\boldsymbol{s}),\boldsymbol{u},\boldsymbol{v})) < 0\right\}\\ &= \left\{\boldsymbol{z}_{\mathcal{C}}(\boldsymbol{s}) : \theta_f \in (0,2\pi),\ \varphi_f \in \left(\frac{\theta_f}{2}-\pi, \frac{\theta_f}{2}\right)\right\}.\end{aligned}$$

The boundary of the usable part ($\mathcal{BUP}$) is a locus of points where the barrier starts its emanation in the backward time. By definition, $\mathcal{BUP} = \partial\mathcal{UP}$. In the GTIC, the boundary of the usable part consists of three lines: $\mathcal{BUP} = \mathcal{BUP}_0 \cup \mathcal{BUP}_{-1} \cup \mathcal{BUP}_{+1}$. The line $\mathcal{BUP}_0$ corresponds to $\theta_f = 0_{\mathbb{S}}$.

$$\mathcal{BUP}_0 \stackrel{\text{def}}{=} \left\{\boldsymbol{z}_{\mathcal{BUP}_0}(\varphi_f) : \varphi_f \in \mathbb{S}\right\} = \{\boldsymbol{z} \in \mathbb{R}^2 \times \mathbb{S} :\ \theta = 0_{\mathbb{S}},\ \ell = \sqrt{x^2+y^2}\},$$

where

$$\boldsymbol{z}_{\mathcal{BUP}_0}(\varphi_f) \stackrel{\text{def}}{=} \boldsymbol{z}_{\mathcal{C}}(\varphi_f, 0_{\mathbb{S}}) = \begin{bmatrix}\ell\sin\varphi_f & \ell\cos\varphi_f & 0_{\mathbb{S}}\end{bmatrix}^\top.$$

For future purposes, we specify the unit normal of the target set on $\mathcal{BUP}_0$.

$$\boldsymbol{n}_{\mathcal{BUP}_0}(\varphi_f) \stackrel{\text{def}}{=} \boldsymbol{n}_{\mathcal{C}}(\varphi_f, 0_{\mathbb{S}}).$$

The last two parts of $\mathcal{BUP}$ correspond to the cases $\varphi_f = \theta_f/2 - \pi$ and $\varphi_f = \theta_f/2$. We denote[1] by $\mathcal{BUP}_\upsilon$ these two lines $\upsilon \in \mathbb{B}$. The parametric description of these lines is given by

$$\mathcal{BUP}_\upsilon \stackrel{\text{def}}{=} \left\{\boldsymbol{z}_{\mathcal{BUP}_\upsilon}(\theta_f) :\ \theta_f \in (0,2\pi)\right\},$$

where

$$\boldsymbol{z}_{\mathcal{BUP}_\upsilon}(\theta_f) \stackrel{\text{def}}{=} \boldsymbol{z}_{\mathcal{C}}\left(\frac{(1+\upsilon)\pi+\theta_f}{2}, \theta_f\right) = \left[-\upsilon\ell\sin\tfrac{\theta_f}{2} \quad -\upsilon\ell\cos\tfrac{\theta_f}{2} \quad \theta_f\right]^\top.$$

The unit normal of the target set on $\mathcal{BUP}_\upsilon$ is defined by

$$\boldsymbol{n}_{\mathcal{BUP}_\upsilon}(\theta_f) \stackrel{\text{def}}{=} \boldsymbol{n}_{\mathcal{C}}\left(\frac{(1+\upsilon)\pi+\theta_f}{2}, \theta_f\right).$$

[1] Throughout the paper, $\mathbb{B}$ denotes the binary set $\{-1,+1\}$. Additionally, we use the letter υ (upsilon) to denote a binary variable. This letter looks like an evader's control v, which will actually play this role.

The emanation of the barrier surface is determined by candidate optimal control laws $\tilde{u}(\cdot)$ and $\tilde{v}(\cdot)$ from Lemma 3.1. Because the values of the candidate optimal control laws may be ambiguous, all the necessary scenarios should be examined. The initial conditions of the retrogressive emanation are given by $\boldsymbol{z}(t_f) = \boldsymbol{z}_{\mathcal{C}}(\boldsymbol{s}) \in \mathcal{BUP}$ and $\nu_{\boldsymbol{z}}(t_f) = \boldsymbol{n}_{\mathcal{C}}(\boldsymbol{s})$. We consider emanation from $\mathcal{BUP}$ separately for $\mathcal{BUP}_0$ and $\mathcal{BUP}_\upsilon$.

4.1 Primary Barrier Emanation

For $\mathcal{BUP}_\upsilon$, the candidate optimal control laws $\tilde{u}(\cdot)$ and $\tilde{v}(\cdot)$ are determined uniquely and according to Lemma 3.1 are equal to

$$\tilde{u}(\boldsymbol{z}_{\mathcal{BUP}_\upsilon}(\theta_f), \boldsymbol{n}_{\mathcal{BUP}_\upsilon}(\theta_f)) = -\upsilon, \quad \tilde{v}(\boldsymbol{z}_{\mathcal{BUP}_\upsilon}(\theta_f), \boldsymbol{n}_{\mathcal{BUP}_\upsilon}(\theta_f)) = \upsilon, \tag{8}$$

where $\theta_f \in (0, 2\pi)$. We associate the notion $\mathcal{B}^\upsilon_{\mathcal{P}}$ with part of the barrier $\mathcal{B}$ that emanates from $\mathcal{BUP}_\upsilon$ (recall that $\upsilon \in \mathbb{B}$). Because not all emanating parts are valid parts of the barrier, we mark the emanating parts with a tilde. Therefore, $\tilde{\mathcal{B}}^\upsilon_{\mathcal{P}}$ emanates from the $\mathcal{BUP}_\upsilon$ and $\mathcal{B}^\upsilon_{\mathcal{P}} = \tilde{\mathcal{B}}^\upsilon_{\mathcal{P}} \cap \mathcal{B}$ is a valid part of the barrier. The redundant part $\tilde{\mathcal{B}}^\upsilon_{\mathcal{P}} \backslash \mathcal{B}^\upsilon_{\mathcal{P}}$ is determined later. Combining (8) with the solution of equations of motion for fixed values of controls (6), we obtain

$$\begin{aligned}
&\boldsymbol{z}_{\mathcal{B}^\upsilon_{\mathcal{P}}}(\tau, \theta_f) \stackrel{\text{def}}{=} \boldsymbol{z}_{-\upsilon,\upsilon}(\tau; \boldsymbol{z}_{\mathcal{BUP}_\upsilon}(\theta_f)) \\
&= \begin{bmatrix} -\upsilon\ell \sin\left(\frac{\theta_f}{2} - \upsilon\tau\right) - \upsilon\left(1 - \cos\tau + \cos(\theta_f - 2\upsilon\tau) - \cos(\theta_f - \upsilon\tau)\right) \\ -\upsilon\ell \cos\left(\frac{\theta_f}{2} - \upsilon\tau\right) + \sin\tau + \upsilon\left(\sin(\theta_f - 2\upsilon\tau) - \sin(\theta_f - \upsilon\tau)\right) \\ \theta_f - 2\upsilon\tau \end{bmatrix}.
\end{aligned}$$

The normal vector of $\tilde{\mathcal{B}}^\upsilon_{\mathcal{P}}$ at $\boldsymbol{z}_{\mathcal{B}^\upsilon_{\mathcal{P}}}(\tau, \theta_f)$ is given by

$$\nu_{\boldsymbol{z},\mathcal{B}^\upsilon_{\mathcal{P}}}(\tau, \theta_f) \stackrel{\text{def}}{=} \nu_{\boldsymbol{z}}^{-\upsilon,\upsilon}(\tau; \boldsymbol{z}_{\mathcal{BUP}_\upsilon}(\theta_f), \boldsymbol{n}_{\mathcal{BUP}_\upsilon}(\theta_f)).$$

The range of change for retrograde time τ on $\tilde{\mathcal{B}}^\upsilon_{\mathcal{P}}$ starts from $\tau = 0$ and ends at an arbitrary moment. This time moment can be defined in such a way that it is guaranteed that it is not less than either the minimal switch time (when one of the switch functions vanishes) or the time when $\tilde{\mathcal{B}}^\upsilon_{\mathcal{P}}$ intersects another part of $\mathcal{B}$. The second option is not available, because the other parts of $\mathcal{B}$ are not described. The computation of the minimal switch time requires finding a minimal positive root of

$$\begin{aligned}
s_P(\boldsymbol{z}_{\mathcal{B}^\upsilon_{\mathcal{P}}}(\tau, \theta_f), \nu_{\boldsymbol{z},\mathcal{B}^\upsilon_{\mathcal{P}}}(\tau, \theta_f)) &= \cos\frac{\theta_f}{2} - \cos\left(\frac{\theta_f}{2} - \upsilon\tau\right) = 0, \\
s_E(\boldsymbol{z}_{\mathcal{B}^\upsilon_{\mathcal{P}}}(\tau, \theta_f), \nu_{\boldsymbol{z},\mathcal{B}^\upsilon_{\mathcal{P}}}(\tau, \theta_f)) &= \cos\left(\frac{\theta_f}{2} - \upsilon\tau\right) - \cos\frac{\theta_f}{2} = 0.
\end{aligned}$$

A trivial verification indicates that the root is $\tau = (1-\upsilon)\pi + \upsilon\theta_f$ for $\theta_f \in (0, 2\pi)$. The third component of $z_{\mathcal{B}^{\upsilon}_{\mathcal{P}}}(\tau, \theta_f)$ becomes zero when

$$\tau = \frac{(1-\upsilon)\pi + \upsilon\theta_f}{2}, \quad \theta_f \in (0, 2\pi),$$

which occurs before the switching function vanishes. Because the evader can escape in the case $\theta = 0_{\mathbb{S}}$ duplicating the strategy of the pursuer, the corresponding state does not belong to $\mathcal{B}$ and lies on the redundant part of $\tilde{\mathcal{B}}^{\upsilon}_{\mathcal{P}}$. Summarizing, we set

$$\tilde{\mathcal{B}}^{\upsilon}_{\mathcal{P}} \stackrel{\text{def}}{=} \left\{ z_{\mathcal{B}^{\upsilon}_{\mathcal{P}}}(\tau, \theta_f) : \ \theta_f \in (0, 2\pi), \ \tau \in \left(0, \frac{(1-\upsilon)\pi + \upsilon\theta_f}{2}\right) \right\}.$$

In the future, we will use another parameterization of $\tilde{\mathcal{B}}^{\upsilon}_{\mathcal{P}}$ given by a new variable $\vartheta = (1-\upsilon)\pi + \upsilon\theta_f - 2\tau$.

$$\tilde{\mathcal{B}}^{\upsilon}_{\mathcal{P}} = \left\{ \bar{z}_{\mathcal{B}^{\upsilon}_{\mathcal{P}}}(\tau, \vartheta) : \ \vartheta \in (0, 2\pi), \ \tau \in \left(0, \pi - \frac{\vartheta}{2}\right) \right\},$$

where

$$\begin{aligned} \bar{z}_{\mathcal{B}^{\upsilon}_{\mathcal{P}}}(\tau, \vartheta) &\stackrel{\text{def}}{=} z_{\mathcal{B}^{\upsilon}_{\mathcal{P}}}(\tau, (1-\upsilon)\pi + \upsilon\vartheta + 2\upsilon\tau) \\ &= \begin{bmatrix} -\upsilon\left(\ell \sin\frac{\vartheta}{2} + \cos\vartheta - \cos(\tau+\vartheta) + 1 - \cos\tau\right) \\ -\ell\cos\frac{\vartheta}{2} + \sin\vartheta - \sin(\tau+\vartheta) + \sin\tau \\ (1-\upsilon)\pi + \upsilon\vartheta \end{bmatrix}. \end{aligned}$$

This parameterization is more convenient, because the third component of the state vector depends only on ϑ.

Let us now turn to emanating from $\mathcal{BUP}_0$. Candidate optimal control laws $\tilde{u}(\cdot)$ and $\tilde{v}(\cdot)$ are equal to

$$\begin{aligned} \tilde{u}(z_{\mathcal{BUP}_0}(\varphi_f), \boldsymbol{n}_{\mathcal{BUP}_0}(\varphi_f)) &= \begin{cases} \operatorname{sgn}\sin\varphi_f, & \varphi_f \neq 0_{\mathbb{S}}; \\ u \in \{-1, 0, +1\}, & \varphi_f = 0_{\mathbb{S}}, \end{cases} \\ \tilde{v}(z_{\mathcal{BUP}_0}(\varphi_f), \boldsymbol{n}_{\mathcal{BUP}_0}(\varphi_f)) &= \begin{cases} \operatorname{sgn}\sin\varphi_f, & \varphi_f \neq 0_{\mathbb{S}}; \\ v \in \{-1, 0, +1\}, & \varphi_f = 0_{\mathbb{S}}. \end{cases} \end{aligned} \tag{9}$$

If $\varphi_f \neq 0_{\mathbb{S}}$, then the controls are equal. Substituting $u = v = \upsilon \in \mathbb{B}$ and $\tilde{z} = z_{\mathcal{BUP}_0}(\varphi_f)$ into (7) yields $r_{\upsilon,\upsilon}(\tau; z_{\mathcal{BUP}_0}(\varphi_f)) = \ell$. This means that the state vector remains on $\mathcal{BUP}_0$ and emanation does not proceed.

Next, if $\varphi_f = 0_{\mathbb{S}}$, then according to (9), we must analyze nine scenarios $u, v \in \{-1, 0, +1\}$. Using Taylor's formula for expression (7), the distance between players is as follows

$$r_{u,v}(\tau; z_{\mathcal{BUP}_0}(0_{\mathbb{S}})) = \ell + \frac{v^2 - u^2}{6}\tau^3 + \frac{(u-v)^2}{8\ell}\tau^4 + o(\tau^4). \tag{10}$$

If $u = v \in \{-1, 0, +1\}$, as in the previous case, then $r_{v,v}(\tau; z_{\mathcal{BUP}_0}(0_{\mathbb{S}})) = \ell$.

Next, if $u \in \mathbb{B}$ and $v = 0$, then according to (10), the distance becomes less than the capture radius at the start of emanation. The region inside the capture circle does not belong to the game set. Consequently, this case can be missed.

Now, let $v = -u = \upsilon \in \mathbb{B}$. We associate the notions $\mathcal{B}^{\upsilon}_{\mathcal{PL}}$ and $\tilde{\mathcal{B}}^{\upsilon}_{\mathcal{PL}}$ with the part of barrier $\mathcal{B}$, that emanates from $\begin{bmatrix} 0 & \ell & 0_{\mathbb{S}} \end{bmatrix}^{\top} \in \mathcal{BUP}_0$ by analogy with $\mathcal{B}^{\upsilon}_{\mathcal{P}}$ and $\tilde{\mathcal{B}}^{\upsilon}_{\mathcal{P}}$ notions. $\tilde{\mathcal{B}}^{\upsilon}_{\mathcal{PL}}$ is a line, whereas $\tilde{\mathcal{B}}^{\upsilon}_{\mathcal{P}}$ is a surface. Similarly, we can describe the points on $\tilde{\mathcal{B}}^{\upsilon}_{\mathcal{PL}}$

$$z_{\mathcal{B}^{\upsilon}_{\mathcal{PL}}}(\tau) \stackrel{\text{def}}{=} z_{-\upsilon,\upsilon}(\tau; z_{\mathcal{BUP}_0}(0_{\mathbb{S}})) = \begin{bmatrix} -\upsilon\,(\ell \sin\tau - 2\cos\tau + 1 + \cos 2\tau) \\ \ell\cos\tau + 2\sin\tau - \sin 2\tau \\ (1+\upsilon)\pi - 2\upsilon\tau \end{bmatrix}$$

and corresponding normal vector

$$\nu_{z,\mathcal{B}^{\upsilon}_{\mathcal{PL}}}(\tau) \stackrel{\text{def}}{=} \nu_z^{-\upsilon,\upsilon}(\tau; z_{\mathcal{BUP}_0}(0_{\mathbb{S}}), \boldsymbol{n}_{\mathcal{BUP}_0}(0_{\mathbb{S}})).$$

The analysis of the switch functions

$$\begin{aligned} s_P(z_{\mathcal{B}^{\upsilon}_{\mathcal{PL}}}(\tau), \nu_z, \mathcal{B}^{\upsilon}_{\mathcal{PL}}(\tau)) &= \upsilon(\cos\tau - 1) = 0, \\ s_E(z_{\mathcal{B}^{\upsilon}_{\mathcal{PL}}}(\tau), \nu_z, \mathcal{B}^{\upsilon}_{\mathcal{PL}}(\tau)) &= \upsilon(1 - \cos\tau) = 0 \end{aligned}$$

gives the minimal switch time $\tau = 2\pi$. The third component of $z_{\mathcal{B}^{\upsilon}_{\mathcal{PL}}}(\tau)$ vanishes at $\tau = \pi$. Therefore, it may be concluded that

$$\tilde{\mathcal{B}}^{\upsilon}_{\mathcal{PL}} \stackrel{\text{def}}{=} \{z_{\mathcal{B}^{\upsilon}_{\mathcal{PL}}}(\tau) : \ \tau \in (0, \pi)\}. \tag{11}$$

Applying a new parametrization $\tau = \pi - \vartheta/2$, we can rewrite (11) as

$$\tilde{\mathcal{B}}^{\upsilon}_{\mathcal{PL}} = \{\bar{z}_{\mathcal{B}^{\upsilon}_{\mathcal{PL}}}(\vartheta) : \ \vartheta \in (0, 2\pi)\},$$

where

$$\bar{z}_{\mathcal{B}^{\upsilon}_{\mathcal{PL}}}(\vartheta) \stackrel{\text{def}}{=} z_{\mathcal{B}^{\upsilon}_{\mathcal{PL}}}\left(\pi - \frac{\vartheta}{2}\right) = \begin{bmatrix} -\upsilon\left(\ell \sin\frac{\vartheta}{2} + 2\cos\frac{\vartheta}{2} + 1 + \cos\vartheta\right) \\ -\ell\cos\frac{\vartheta}{2} + 2\sin\frac{\vartheta}{2} + \sin\vartheta \\ (1-\upsilon)\pi + \upsilon\vartheta \end{bmatrix}.$$

A simple computation shows that $\bar{z}_{\mathcal{B}^{\upsilon}_{\mathcal{P}}}(\vartheta, \pi - \vartheta/2) = \bar{z}_{\mathcal{B}^{\upsilon}_{\mathcal{PL}}}(\vartheta)$ for all $\vartheta \in (0, 2\pi)$, which implies that $\tilde{\mathcal{B}}^{\upsilon}_{\mathcal{PL}}$ is part of the boundary of $\tilde{\mathcal{B}}^{\upsilon}_{\mathcal{P}}$.

Finally, we consider the case $u = 0$ and $v = \upsilon \in \mathbb{B}$. We will see later that this case corresponds to the emanation of barrier universal line. The notations $\mathcal{B}^{\upsilon}_{\mathcal{UL}}$ and $\tilde{\mathcal{B}}^{\upsilon}_{\mathcal{UL}}$

are associated with the emanation. The points of $\tilde{\mathcal{B}}^{\upsilon}_{\mathcal{UL}}$ are given by

$$z_{\mathcal{B}^{\upsilon}_{\mathcal{UL}}}(\tau) \stackrel{\text{def}}{=} z_{0,\upsilon}(\tau; z_{\mathcal{BUP}_0}(0_{\mathbb{S}})) = \begin{bmatrix} \upsilon(1-\cos\tau) \\ \ell + \tau - \sin\tau \\ (1+\upsilon)\pi - \upsilon\tau \end{bmatrix}.$$

The normal vector is defined by

$$\nu_{z,\mathcal{B}^{\upsilon}_{\mathcal{UL}}}(\tau) \stackrel{\text{def}}{=} \nu_z^{0,\upsilon}(\tau; z_{\mathcal{BUP}_0}(0_{\mathbb{S}}), \boldsymbol{n}_{\mathcal{BUP}_0}(0_{\mathbb{S}})) = \begin{bmatrix} 0 \\ 1 \\ \upsilon(1-\cos\tau) \end{bmatrix}. \tag{12}$$

Computing the switch functions on $\tilde{\mathcal{B}}^{\upsilon}_{\mathcal{UL}}$ gives

$$s_P(z_{\mathcal{B}^{\upsilon}_{\mathcal{UL}}}(\tau), \nu_{z,\mathcal{B}^{\upsilon}_{\mathcal{UL}}}(\tau)) = 0, \quad s_E(z_{\mathcal{B}^{\upsilon}_{\mathcal{UL}}}(\tau), \nu_{z,\mathcal{B}^{\upsilon}_{\mathcal{UL}}}(\tau)) = \upsilon(1-\cos\tau).$$

Because the first component of (12) is equal to zero and the second component is non-negative, emanation with $u \in \{-1, 0, +1\}$ is not prohibited on $\tilde{\mathcal{B}}^{\upsilon}_{\mathcal{UL}}$ (according to Lemma 3.1). The minimum switch time of the evader switch function is $\tau = 2\pi$. Thus,

$$\tilde{\mathcal{B}}^{\upsilon}_{\mathcal{UL}} \stackrel{\text{def}}{=} \{z_{\mathcal{B}^{\upsilon}_{\mathcal{UL}}}(\tau) : \ \tau \in (0, 2\pi)\}.$$

For the uniformity of notation, we define $\bar{z}_{\mathcal{B}^{\upsilon}_{\mathcal{UL}}}(\vartheta) = z_{\mathcal{B}^{\upsilon}_{\mathcal{UL}}}(\vartheta)$.

Thus, the primary emanation of trajectories from $\mathcal{BUP}$ is exhausted by two surfaces $\tilde{\mathcal{B}}^{\upsilon}_{\mathcal{P}}$ and four lines $\tilde{\mathcal{B}}^{\upsilon}_{\mathcal{PL}}$, $\tilde{\mathcal{B}}^{\upsilon}_{\mathcal{UL}}$ ($\upsilon \in \mathbb{B}$). Simultaneously, each line $\tilde{\mathcal{B}}^{\upsilon}_{\mathcal{PL}}$ corresponds to the boundary of the surface $\tilde{\mathcal{B}}^{\upsilon}_{\mathcal{P}}$. Next, we describe the tributaries of $\tilde{\mathcal{B}}^{\upsilon}_{\mathcal{UL}}$, which consist of retrograde trajectories emanating in a retrograde sense from this line.

4.2 Tributaries Emanation

We explore the emanation in two scenarios, since the tributaries emanate from $\tilde{\mathcal{B}}^{\upsilon}_{\mathcal{UL}}$ with two possible values for the pursuer control $u \in \mathbb{B}$. In the first scenario, we assume that players' controls are equal and that the players turn in the same direction. In the second scenario, the players turn in opposite directions. That is, the controls of the players are different.

We associate the notions $\mathcal{B}^{\upsilon}_{\mathcal{PL}}$ and $\tilde{\mathcal{B}}^{\upsilon}_{\mathcal{PL}}$ with the emanation of tributaries with the equal control of players. Substituting $u = v = \upsilon \in \mathbb{B}$ into the solution of equations of motion for fixed values of controls, we have

$$z_{\mathcal{B}^{\upsilon}_{\mathcal{TS}}}(\tau_1, \tau_2) \stackrel{\text{def}}{=} z_{\upsilon,\upsilon}(\tau_2; z_{\mathcal{B}^{\upsilon}_{\mathcal{UL}}}(\tau_1)) = \begin{bmatrix} \upsilon\left((\ell+\tau_1)\sin\tau_2 + 1 - \cos\tau_1\right) \\ (\ell+\tau_1)\cos\tau_2 - \sin\tau_1 \\ (1+\upsilon)\pi - \upsilon\tau_1 \end{bmatrix}.$$

Here, $\tau_1 \in (0, 2\pi)$ is the time spent on $\tilde{\mathcal{B}}^{\upsilon}_{\mathcal{UL}}$ and τ_2 is spent on the tributary path. The normal vector is defined by

$$\nu_{z,\mathcal{B}^{\upsilon}_{\mathcal{TS}}}(\tau_1, \tau_2) \stackrel{\text{def}}{=} \nu_z^{\upsilon,\upsilon}(\tau_2; z_{\mathcal{B}^{\upsilon}_{\mathcal{UL}}}(\tau_1), \nu_{z,\mathcal{B}^{\upsilon}_{\mathcal{UL}}}(\tau_1)).$$

Computing the switch functions on $\tilde{\mathcal{B}}^{\upsilon}_{\mathcal{PL}}$ gives

$$\begin{aligned} s_P(z_{\mathcal{B}^{\upsilon}_{\mathcal{TS}}}(\tau_1, \tau_2), \nu_{z,\mathcal{B}^{\upsilon}_{\mathcal{TS}}}(\tau_1, \tau_2)) &= \upsilon(1 - \cos\tau_2) = 0, \\ s_E(z_{\mathcal{B}^{\upsilon}_{\mathcal{TS}}}(\tau_1, \tau_2), \nu_{z,\mathcal{B}^{\upsilon}_{\mathcal{TS}}}(\tau_1, \tau_2)) &= \upsilon\,(1 - \cos\,(\tau_1 + \tau_2)) = 0. \end{aligned}$$

The minimal positive solution of these equations $\tau_2 = 2\pi - \tau_1$ corresponds to zero of the evader switch function. Hence,

$$\tilde{\mathcal{B}}^{\upsilon}_{\mathcal{PL}} \stackrel{\text{def}}{=} \left\{ z_{\mathcal{B}^{\upsilon}_{\mathcal{TS}}}(\tau_1, \tau_2) :\ \tau_1 \in (0, 2\pi)\,,\ \tau_2 \in (0, 2\pi - \tau_1) \right\}.$$

Using a new parameterization, $\tau_1 = \vartheta$ and $\tau_2 = \tau - \vartheta$ we can rewrite the above as

$$\tilde{\mathcal{B}}^{\upsilon}_{\mathcal{PL}} = \left\{ \bar{z}_{\mathcal{B}^{\upsilon}_{\mathcal{TS}}}(\tau, \vartheta) :\ \vartheta \in (0, 2\pi)\,,\ \tau \in (\vartheta, 2\pi) \right\},$$

where

$$\bar{z}_{\mathcal{B}^{\upsilon}_{\mathcal{TS}}}(\tau, \vartheta) \stackrel{\text{def}}{=} z_{\mathcal{B}^{\upsilon}_{\mathcal{TS}}}(\vartheta, \tau - \vartheta) = \begin{bmatrix} \upsilon\,((\ell + \vartheta)\sin(\tau - \vartheta) + 1 - \cos\vartheta) \\ (\ell + \vartheta)\cos(\tau - \vartheta) - \sin\vartheta \\ (1 + \upsilon)\pi - \upsilon\vartheta \end{bmatrix}.$$

Note that $\tau = \tau_1 + \tau_2$ has a sense of the time-to-go to $\mathcal{BUP}_0$.

Next, we associate the notions $\mathcal{B}^{\upsilon}_{\mathcal{TD}}$ and $\tilde{\mathcal{B}}^{\upsilon}_{\mathcal{TD}}$ with the emanation of tributaries with different values of players' controls. Substituting $\upsilon = -u = \upsilon \in \mathbb{B}$ into the solution of the equations of motion, we obtain

$$\begin{aligned} z_{\mathcal{B}^{\upsilon}_{\mathcal{TD}}}(\tau_1, \tau_2) &\stackrel{\text{def}}{=} z_{-\upsilon,\upsilon}(\tau_2; z_{\mathcal{B}^{\upsilon}_{\mathcal{UL}}}(\tau_1)) \\ &= \begin{bmatrix} \upsilon\,(-(\ell + \tau_1)\sin\tau_2 + 2\cos\tau_2 - \cos(\tau_1 + 2\tau_2) - 1) \\ (\ell + \tau_1)\cos\tau_2 + 2\sin\tau_2 - \sin(\tau_1 + 2\tau_2) \\ (1 + \upsilon)\pi - \upsilon(\tau_1 + 2\tau_2) \end{bmatrix}. \end{aligned}$$

The variables τ_1 and τ_2 have the same meaning as in the previous case. The normal vector is

$$\nu_{z,\mathcal{B}^{\upsilon}_{\mathcal{TD}}}(\tau_1, \tau_2) \stackrel{\text{def}}{=} \nu_z^{-\upsilon,\upsilon}(\tau_2; z_{\mathcal{B}^{\upsilon}_{\mathcal{UL}}}(\tau_1), \nu_{z,\mathcal{B}^{\upsilon}_{\mathcal{UL}}}(\tau_1)).$$

Calculation of the switch functions yields

$$\begin{aligned} s_P(z_{\mathcal{B}^{\upsilon}_{\mathcal{TD}}}(\tau_1, \tau_2), \nu_{z,\mathcal{B}^{\upsilon}_{\mathcal{TD}}}(\tau_1, \tau_2)) &= \upsilon(\cos\tau_2 - 1) = 0, \\ s_E(z_{\mathcal{B}^{\upsilon}_{\mathcal{TD}}}(\tau_1, \tau_2), \nu_{z,\mathcal{B}^{\upsilon}_{\mathcal{TD}}}(\tau_1, \tau_2)) &= \upsilon\,(1 - \cos\,(\tau_1 + \tau_2)) = 0. \end{aligned}$$

The minimal positive $\tau_2 = 2\pi - \tau_1$ also corresponds to zero in the evader switch function, but the third component of $z_{\mathcal{B}^{\upsilon}_{\mathcal{TD}}}(\tau_1, \tau_2)$ vanishes earlier at $\tau_2 = \pi - \tau_1/2$. Therefore, we set

$$\tilde{\mathcal{B}}^{\upsilon}_{\mathcal{TD}} \stackrel{\text{def}}{=} \left\{ z_{\mathcal{B}^{\upsilon}_{\mathcal{TD}}}(\tau_1, \tau_2) : \ \tau_1 \in (0, 2\pi), \ \tau_2 \in \left(0, \pi - \frac{\tau_1}{2}\right) \right\}.$$

Using a new parameterization, $\tau_1 = 2\tau - \vartheta$ and $\tau_2 = \vartheta - \tau$ we obtain

$$\tilde{\mathcal{B}}^{\upsilon}_{\mathcal{TD}} = \left\{ \bar{z}_{\mathcal{B}^{\upsilon}_{\mathcal{TD}}}(\tau, \vartheta) : \ \vartheta \in (0, 2\pi), \ \tau \in \left(\frac{\vartheta}{2}, \vartheta\right) \right\},$$

where

$$\begin{aligned} \bar{z}_{\mathcal{B}^{\upsilon}_{\mathcal{TD}}}(\tau, \vartheta) &\stackrel{\text{def}}{=} z_{\mathcal{B}^{\upsilon}_{\mathcal{TD}}}(2\tau - \vartheta, \vartheta - \tau) \\ &= \begin{bmatrix} \upsilon\left((\ell + 2\tau - \vartheta)\sin(\tau - \vartheta) + 2\cos(\tau - \vartheta) - 1 - \cos\vartheta\right) \\ (\ell + 2\tau - \vartheta)\cos(\tau - \vartheta) - 2\sin(\tau - \vartheta) - \sin\vartheta \\ (1 + \upsilon)\pi - \upsilon\vartheta \end{bmatrix}. \end{aligned}$$

A simple computation shows that $\bar{z}_{\mathcal{B}^{\upsilon}_{\mathcal{TD}}}(\vartheta/2, \vartheta) = \bar{z}_{\mathcal{B}^{\upsilon}_{\mathcal{PL}}}(2\pi - \vartheta)$ for all $\vartheta \in (0, 2\pi)$, proving that the line $\tilde{\mathcal{B}}^{\upsilon}_{\mathcal{PL}}$ is a part of the boundary of the surface $\tilde{\mathcal{B}}^{\upsilon}_{\mathcal{TD}}$.

4.3 Barrier Self-Intersections

The description provided above is a convenient presentation of the key results from [17, 25]. Further analysis refines these results and leads to explicit analytical expressions for optimal feedback controls.

We now turn to the problem of determining "redundant" parts of obtained semipermeable surfaces. These "redundant" parts are semipermeable, but they are not involved in the barrier $\mathcal{B}$. The GTIC has symmetry $(x, y, \theta, u, \upsilon) \leftrightarrow (-x, y, 2\pi - \theta, -u, -\upsilon)$, that is, the equations of motion (1) and the capture set $\mathcal{C}$ hold when we use this replacement of variables. This fact admits exploration of the GTIC only for $\theta \in (0, \pi]$. For the rest of the values $\theta \in (\pi, 2\pi)$, we can use this symmetry.

A graphical analysis of the θ-slices of the emanating parts (see Fig. 2) shows that, for sufficiently small values of the capture radius ℓ (e.g., for $\ell = 1/2$), the surface $\tilde{\mathcal{B}}^{\upsilon}_{\mathcal{P}}$ crosses $\tilde{\mathcal{B}}^{-\upsilon}_{\mathcal{TD}}$, but the surface $\tilde{\mathcal{B}}^{\upsilon}_{\mathcal{TD}}$ does not cross $\tilde{\mathcal{B}}^{-\upsilon}_{\mathcal{TS}}$. However, at the same time, for sufficiently large values of ℓ (e.g., for $\ell = 1$), we observe the opposite behavior. This fact suggests the existence of an intermediate value of $\ell = \ell_J$ when the surface $\tilde{\mathcal{B}}^{\upsilon}_{\mathcal{P}}$ does not cross $\tilde{\mathcal{B}}^{-\upsilon}_{\mathcal{TD}}$ and $\tilde{\mathcal{B}}^{\upsilon}_{\mathcal{TD}}$ does not cross $\tilde{\mathcal{B}}^{-\upsilon}_{\mathcal{TS}}$, but the boundaries of these surfaces share a common point for some $\theta = (1 - \upsilon)\pi + \upsilon\vartheta_J$, where $\vartheta_J \in (0, \pi)$ (see Fig. 3).

Lemma 4.1 *There is only one value of the capture radius $\ell = \ell_J$ when line $\tilde{\mathcal{B}}^{\upsilon}_{\mathcal{PL}}$ crosses line $\tilde{\mathcal{B}}^{-\upsilon}_{\mathcal{UL}}$.*

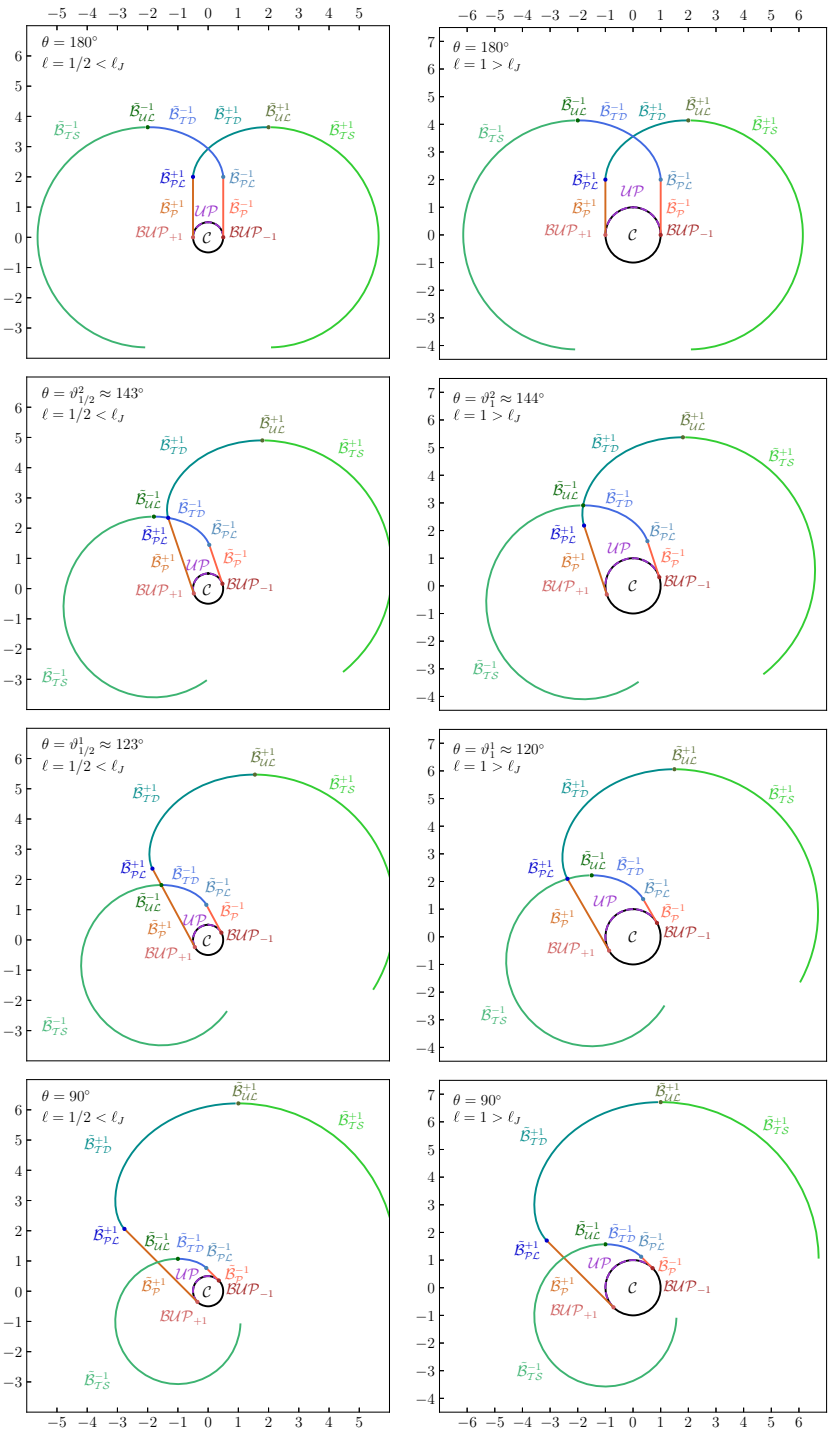

Fig. 2 Cross sections of the emanated surfaces for the small and large capture radius

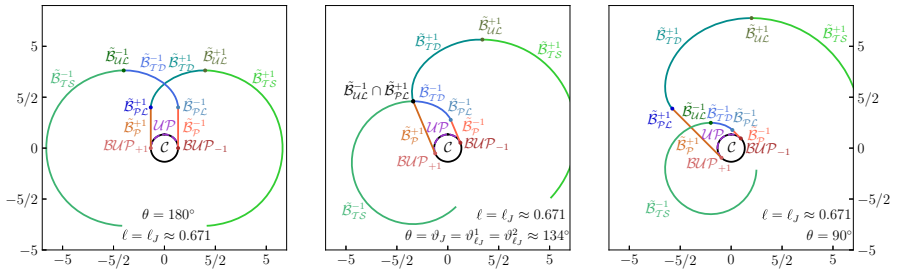

Fig. 3 Cross sections of the emanated surfaces for the medium capture radius $\ell = \ell_J$

For future purposes, we introduce a special rotation matrix

$$\boldsymbol{R}_{\upsilon}(\alpha) \stackrel{\text{def}}{=} \begin{bmatrix} -\upsilon\cos\alpha & \sin\alpha & 0 \\ \upsilon\sin\alpha & \cos\alpha & 0 \\ 0 & 0 & 1 \end{bmatrix}, \quad \alpha \in \mathbb{S}, \quad \upsilon \in \mathbb{B}.$$

Note that, for all $\upsilon \in \mathbb{B}$ and $\alpha \in \mathbb{S}$ this matrix is non-singular. We also use the following functions:

$$\xi_{\ell}(\alpha) \stackrel{\text{def}}{=} (\ell + \alpha)\sin\frac{\alpha}{2} + 2\cos\frac{\alpha}{2}, \quad \eta_{\ell}(\alpha) \stackrel{\text{def}}{=} (\ell + \alpha)\cos\frac{\alpha}{2} - 2\sin\frac{\alpha}{2}.$$

Proof We first prove that system

$$\bar{z}_{\mathcal{B}^{-\upsilon}_{\mathcal{UL}}}(\vartheta) - \bar{z}_{\mathcal{B}^{\upsilon}_{\mathcal{PL}}}(\vartheta) = \mathbf{0}, \quad \vartheta \in (0, 2\pi), \quad \ell \in \mathbb{R}^{+}$$

has only one solution for each $\upsilon \in \mathbb{B}$. By applying $\boldsymbol{R}_{\upsilon}(\vartheta/2)$, we can rewrite this as follows:

$$\boldsymbol{R}_{\upsilon}\left(\frac{\vartheta}{2}\right)\left(\bar{z}_{\mathcal{B}^{-\upsilon}_{\mathcal{UL}}}(\vartheta) - \bar{z}_{\mathcal{B}^{\upsilon}_{\mathcal{PL}}}(\vartheta)\right) = \begin{bmatrix} \xi_{\ell}(\vartheta) - 2 - 4\cos\frac{\vartheta}{2} \\ \eta_{\ell}(\vartheta) + \ell \\ 0_{\mathbb{S}} \end{bmatrix} = \mathbf{0}.$$

Eliminating the variable ℓ from the system yields

$$\vartheta - 4\left(1 + \cos\frac{\vartheta}{2}\right)\cot\frac{\vartheta}{2} = 0, \quad \vartheta \in (0, 2\pi). \tag{13}$$

The left part of (13) approaches $-\infty$ as $\vartheta \to +0$ and 2π as $\vartheta \to 2\pi - 0$. The derivative of the left part equals

$$1 + 2\left(\cos\frac{\vartheta}{2} + \frac{1 + \cos\frac{\vartheta}{2}}{\sin^2\frac{\vartheta}{2}}\right) = \frac{\left(1 + \cos\frac{\vartheta}{2}\right)^2\left(3 - 2\cos\frac{\vartheta}{2}\right)}{\sin^2\frac{\vartheta}{2}} > 0, \quad \vartheta \in (0, 2\pi).$$

Thus, the left-hand side of (13) is a continuous monotonic function. It has the opposite signs for $\vartheta \to +0$ and $\vartheta \to 2\pi - 0$. Hence, Eq. (13) has only one root. □

Applying Newton's method gives the value $\vartheta_J \approx 2.343 \approx 134°$ for the root. The corresponding capture radius is given by

$$\ell_J \stackrel{\text{def}}{=} -2\frac{\cos\frac{\vartheta_J}{2} + \cos\vartheta_J}{\sin\frac{\vartheta_J}{2}} \approx 0.671.$$

The intersection of the semipermeable surfaces constituting the barrier indicates the presence of a dispersal line on the barrier. Analysis of θ-slices in Figs. 2–3 shows that the dispersal line is built in different ways, depending on the value of the capture radius ℓ. Simultaneously, for values of θ close to $0_{\mathbb{S}}$ for all values of the capture radius, there is an intersection $\tilde{\mathcal{B}}^{\upsilon}_{\mathcal{P}} \cap \tilde{\mathcal{B}}^{-\upsilon}_{\mathcal{TS}}$, and for θ close to π there is an intersection $\tilde{\mathcal{B}}^{\upsilon}_{\mathcal{TD}} \cap \tilde{\mathcal{B}}^{-\upsilon}_{\mathcal{TD}}$. We used the notation $\mathcal{B}_{\mathcal{DL}}$ for the dispersal line. Taking into account all of these facts, we distinguish three cases of constructing a dispersal line:

– The small capture radius $\ell \in (0, \ell_J)$

$$\mathcal{B}_{\mathcal{DL}} \stackrel{\text{def}}{=} \bigcup_{\upsilon\in\mathbb{B}} \Big[\Big(\tilde{\mathcal{B}}^{\upsilon}_{\mathcal{P}} \cap \tilde{\mathcal{B}}^{-\upsilon}_{\mathcal{TS}}\Big) \cup \Big(\tilde{\mathcal{B}}^{\upsilon}_{\mathcal{P}} \cap \tilde{\mathcal{B}}^{-\upsilon}_{\mathcal{UL}}\Big) \cup \Big(\tilde{\mathcal{B}}^{\upsilon}_{\mathcal{P}} \cap \tilde{\mathcal{B}}^{-\upsilon}_{\mathcal{TD}}\Big) \cup \Big(\tilde{\mathcal{B}}^{\upsilon}_{\mathcal{PL}} \cap \tilde{\mathcal{B}}^{-\upsilon}_{\mathcal{TD}}\Big) \cup \Big(\tilde{\mathcal{B}}^{\upsilon}_{\mathcal{TD}} \cap \tilde{\mathcal{B}}^{-\upsilon}_{\mathcal{TD}}\Big)\Big],$$

– The medium capture radius $\ell = \ell_J$

$$\mathcal{B}_{\mathcal{DL}} \stackrel{\text{def}}{=} \bigcup_{\upsilon\in\mathbb{B}} \Big[\Big(\tilde{\mathcal{B}}^{\upsilon}_{\mathcal{P}} \cap \tilde{\mathcal{B}}^{-\upsilon}_{\mathcal{TS}}\Big) \cup \Big(\tilde{\mathcal{B}}^{\upsilon}_{\mathcal{PL}} \cap \tilde{\mathcal{B}}^{-\upsilon}_{\mathcal{UL}}\Big) \cup \Big(\tilde{\mathcal{B}}^{\upsilon}_{\mathcal{TD}} \cap \tilde{\mathcal{B}}^{-\upsilon}_{\mathcal{TD}}\Big)\Big],$$

– The large capture radius $\ell \in (\ell_J, +\infty)$

$$\mathcal{B}_{\mathcal{DL}} \stackrel{\text{def}}{=} \bigcup_{\upsilon\in\mathbb{B}} \Big[\Big(\tilde{\mathcal{B}}^{\upsilon}_{\mathcal{P}} \cap \tilde{\mathcal{B}}^{-\upsilon}_{\mathcal{TS}}\Big) \cup \Big(\tilde{\mathcal{B}}^{\upsilon}_{\mathcal{PL}} \cap \tilde{\mathcal{B}}^{-\upsilon}_{\mathcal{TS}}\Big) \cup \Big(\tilde{\mathcal{B}}^{\upsilon}_{\mathcal{TD}} \cap \tilde{\mathcal{B}}^{-\upsilon}_{\mathcal{TS}}\Big) \cup \Big(\tilde{\mathcal{B}}^{\upsilon}_{\mathcal{TD}} \cap \tilde{\mathcal{B}}^{-\upsilon}_{\mathcal{UL}}\Big) \cup \Big(\tilde{\mathcal{B}}^{\upsilon}_{\mathcal{TD}} \cap \tilde{\mathcal{B}}^{-\upsilon}_{\mathcal{TD}}\Big)\Big].$$

To determine which range of θ corresponds to the intersection $\tilde{\mathcal{B}}^{\upsilon}_{\mathcal{P}} \cap \tilde{\mathcal{B}}^{-\upsilon}_{\mathcal{TS}}$, we must find the critical value of the angle at which the universal line $\tilde{\mathcal{B}}^{-\upsilon}_{\mathcal{UL}}$ crosses the surface $\tilde{\mathcal{B}}^{\upsilon}_{\mathcal{P}}$ if ℓ is small. If ℓ is large, then the critical value of the angle corresponds to the intersection of line $\tilde{\mathcal{B}}^{\upsilon}_{\mathcal{PL}}$ with the surface $\tilde{\mathcal{B}}^{-\upsilon}_{\mathcal{TS}}$. For the medium value of ℓ, the critical value of the angle is $(1-\upsilon)\pi + \upsilon\vartheta_J$. We denote by ϑ^1_ℓ the dependence of the critical value of the angle from the capture radius ℓ for $\upsilon = +1$. If $\upsilon = -1$, this angle is equal to $2\pi - \vartheta^1_\ell$ owing to the symmetry of the problem. Next, we will calculate these intersections.

The intersection of $\tilde{\mathcal{B}}^{-\upsilon}_{\mathcal{UL}}$ with $\tilde{\mathcal{B}}^{\upsilon}_{\mathcal{P}}$ is given by the system and interval constraints

$$\bar{z}_{\mathcal{B}^{-\upsilon}_{\mathcal{UL}}}(\vartheta) = \bar{z}_{\mathcal{B}^{\upsilon}_{\mathcal{P}}}(\tau, \vartheta), \quad \vartheta \in (0, 2\pi), \quad \tau \in \left(0, \pi - \frac{\vartheta}{2}\right), \quad \ell \in (0, \ell_J).$$

A unique solution to the system for the given ranges of ϑ and τ is

$$\tau = -\frac{w_\ell}{2} + \arccos\left(2\cos\frac{w_\ell}{2} - \frac{\sqrt{(\ell + w_\ell)^2 - \ell^2 + 4}}{2}\right), \quad \vartheta = w_\ell,$$

where w_ℓ is the root of the transcendental equation

$$\eta_\ell(w) + \ell = 0, \quad w \in (0, 2\pi), \quad \ell \in (0, \ell_J).$$

The intersection of $\tilde{\mathcal{B}}^{\upsilon}_{\mathcal{PL}}$ with $\tilde{\mathcal{B}}^{-\upsilon}_{\mathcal{TS}}$ is determined by the system and interval constraints

$$\bar{z}_{\mathcal{B}^{-\upsilon}_{\mathcal{TS}}}(\tau, \vartheta) = \bar{z}_{\mathcal{B}^{\upsilon}_{\mathcal{PL}}}(\vartheta), \quad \vartheta \in (0, 2\pi), \quad \tau \in (\vartheta, 2\pi), \quad \ell \in (\ell_J, +\infty).$$

A unique solution to the above system for the given ranges of ϑ and τ is

$$\tau = \pi - \arccos\frac{\ell\cos\frac{m_\ell}{2} + 2\sin\frac{m_\ell}{2}}{\ell + m_\ell}, \quad \vartheta = m_\ell.$$

Here, m_ℓ is the root of the transcendental equation

$$(\ell + m)^2 - \left(2\sin\frac{m}{2} - \ell\right)^2 - \left(2 + 2\cos\frac{m}{2}\right)^2 = 0, \quad m \in (0, 2\pi), \quad \ell \in (\ell_J, +\infty).$$

Summarizing, we obtain the critical value of angle given by

$$\vartheta^1_\ell \stackrel{\text{def}}{=} \begin{cases} w_\ell, & \ell \in (0, \ell_J), \\ \vartheta_J, & \ell = \ell_J, \\ m_\ell, & \ell \in (\ell_J, +\infty). \end{cases}$$

Similarly, we can determine the range of θ corresponding to the intersection $\tilde{\mathcal{B}}^{\upsilon}_{\mathcal{TD}} \cap \tilde{\mathcal{B}}^{-\upsilon}_{\mathcal{TD}}$. Now we must find the critical value of the angle at which the line $\tilde{\mathcal{B}}^{\upsilon}_{\mathcal{PL}}$ crosses the surface $\tilde{\mathcal{B}}^{-\upsilon}_{\mathcal{TD}}$ if ℓ is small. If ℓ is large, then the critical value of the angle corresponds to the intersection of the universal line $\tilde{\mathcal{B}}^{-\upsilon}_{\mathcal{UL}}$ with the surface $\tilde{\mathcal{B}}^{\upsilon}_{\mathcal{TD}}$. For the medium value of ℓ, the critical value of the angle is $(1 - \upsilon)\pi + \upsilon\vartheta_J$. Similarly, we denote by ϑ^2_ℓ the dependence of the critical value of the angle from the capture radius ℓ for $\upsilon = +1$. If $\upsilon = -1$, this angle is equal to $2\pi - \vartheta^2_\ell$.

The intersection of $\tilde{\mathcal{B}}^{\upsilon}_{\mathcal{PL}}$ with $\tilde{\mathcal{B}}^{-\upsilon}_{\mathcal{TD}}$ is given by the system

$$\bar{z}_{\mathcal{B}^{-\upsilon}_{\mathcal{TD}}}(\tau,\vartheta)=\bar{z}_{\mathcal{B}^{\upsilon}_{\mathcal{PL}}}(\vartheta),\quad \vartheta\in(0,2\pi),\quad \tau\in\left(\frac{\vartheta}{2},\vartheta\right),\quad \ell\in(0,\ell_J).$$

A unique solution to the system for the given ranges of ϑ and τ is

$$\tau=\frac{w_\ell}{2}+\arccos\frac{\sqrt{(\ell+w_\ell)^2-\ell^2+4}-2}{4},\ \vartheta=2\arccos\frac{\sqrt{(\ell+w_\ell)^2-\ell^2+4}-2}{4}.$$

The intersection of $\tilde{\mathcal{B}}^{-\upsilon}_{\mathcal{UL}}$ with $\tilde{\mathcal{B}}^{\upsilon}_{\mathcal{TD}}$ is determined by the system

$$\begin{aligned}&\bar{z}_{\mathcal{B}^{-\upsilon}_{\mathcal{UL}}}(\vartheta)=\bar{z}_{\mathcal{B}^{\upsilon}_{\mathcal{TD}}}(\tau,2\pi-\vartheta),\quad \vartheta\in(0,2\pi),\\ &\tau\in\left(\pi-\frac{\vartheta}{2},2\pi-\vartheta\right),\quad \ell\in(\ell_J,+\infty).\end{aligned}$$

A unique solution to the system for the given ranges of ϑ and τ is

$$\tau=\pi-\frac{\ell+n_\ell}{2}+\frac{\sqrt{(\ell+n_\ell-2\sin n_\ell)^2-4\sin^2 n_\ell}}{2},\quad \vartheta=n_\ell.$$

Here n_ℓ is the root of the transcendental equation

$$\eta_\ell\left(\sqrt{(\ell+n-2\sin n)^2-4\sin^2 n}-\ell\right)+\eta_\ell(n)=0,\quad n\in(0,2\pi),\quad \ell\in(\ell_J,+\infty).$$

Summarizing, we obtain the critical value of angle given by

$$\vartheta^2_\ell\overset{\text{def}}{=}\begin{cases}2\arccos\frac{\sqrt{(\ell+w_\ell)^2-\ell^2+4}-2}{4}, & \ell\in(0,\ell_J);\\ \vartheta_J, & \ell=\ell_J;\\ n_\ell, & \ell\in(\ell_J,+\infty).\end{cases}$$

The critical values of the angles ϑ^1_ℓ and ϑ^2_ℓ provide valid ranges of θ for the computation of intersections $\tilde{\mathcal{B}}^{\upsilon}_{\mathcal{P}}\cap\tilde{\mathcal{B}}^{-\upsilon}_{\mathcal{TS}}$ and $\tilde{\mathcal{B}}^{\upsilon}_{\mathcal{TD}}\cap\tilde{\mathcal{B}}^{-\upsilon}_{\mathcal{TD}}$, respectively. Moreover, for $\upsilon=+1$ an interval $(\vartheta^1_\ell,\vartheta^2_\ell)$ gives the range of θ where the surface $\tilde{\mathcal{B}}^{\upsilon}_{\mathcal{P}}$ crosses $\tilde{\mathcal{B}}^{-\upsilon}_{\mathcal{TD}}$ if ℓ is small and the surface $\tilde{\mathcal{B}}^{\upsilon}_{\mathcal{TD}}$ crosses the $\tilde{\mathcal{B}}^{-\upsilon}_{\mathcal{TS}}$ if ℓ is large (see Fig. 2). For $\upsilon=-1$, the interval is $(2\pi-\vartheta^2_\ell,2\pi-\vartheta^1_\ell)$.

The surface $\tilde{\mathcal{B}}^{-\upsilon}_{\mathcal{TS}}$ crosses $\tilde{\mathcal{B}}^{\upsilon}_{\mathcal{P}}$ when parameter $\vartheta\in(0,\vartheta^1_\ell)$. We use the notation τ' for the parameterization of $\tilde{\mathcal{B}}^{-\upsilon}_{\mathcal{TS}}$ to distinguish between the parameter τ of $\tilde{\mathcal{B}}^{\upsilon}_{\mathcal{P}}$. The intersection is given by

$$\bar{z}_{\mathcal{B}^{-\upsilon}_{\mathcal{TS}}}\left(\tau',\vartheta\right)=\bar{z}_{\mathcal{B}^{\upsilon}_{\mathcal{P}}}\left(\tau,\vartheta\right),\quad \vartheta\in(0,\vartheta^1_\ell),\quad \tau\in\left(0,\pi-\frac{\vartheta}{2}\right),\quad \tau'\in(\vartheta,2\pi).$$

For $\vartheta \in (0, \vartheta_\ell^1)$, a unique solution to the system for the given ranges of τ and τ' is

$$\begin{aligned} \tau &= -\frac{\vartheta}{2} + \arccos\left(\cos\frac{\vartheta}{2} - \frac{1}{2}\sqrt{(\ell+\vartheta)^2 - \left(\ell - 2\sin\frac{\vartheta}{2}\right)^2}\right), \\ \tau' &= \frac{\vartheta}{2} + \arccos\frac{2\sin\frac{\vartheta}{2} - \ell}{\ell+\vartheta}. \end{aligned} \tag{14}$$

Similarly, the intersection of $\tilde{\mathcal{B}}^{\upsilon}_{\mathcal{TD}}$ and $\tilde{\mathcal{B}}^{-\upsilon}_{\mathcal{TD}}$ is given by the system

$$\begin{aligned} &\bar{z}_{\mathcal{B}^{-\upsilon}_{\mathcal{TD}}}(\tau,\vartheta) = \bar{z}_{\mathcal{B}^{\upsilon}_{\mathcal{TD}}}\left(\tau', 2\pi - \vartheta\right),\ \vartheta \in (\vartheta_\ell^2, 2\pi - \vartheta_\ell^2),\ \tau \in \left(\frac{\vartheta}{2}, \vartheta\right), \\ &\tau' \in \left(\pi - \frac{\vartheta}{2}, 2\pi - \vartheta\right). \end{aligned}$$

The parameter τ relates to $\tilde{\mathcal{B}}^{-\upsilon}_{\mathcal{TD}}$ and τ' to $\tilde{\mathcal{B}}^{\upsilon}_{\mathcal{TD}}$. For $\vartheta \in (\vartheta_\ell^2, 2\pi - \vartheta_\ell^2)$, a unique solution to the system for the given ranges of τ and τ' is

$$\begin{aligned} \tau = \frac{\vartheta + p_\ell(\vartheta)}{2},\ \tau' = \pi - \frac{\ell+\vartheta}{2} \\ + \frac{1}{2}\sqrt{\left(\xi_\ell(p_\ell(\vartheta)) - 4\cos\frac{\vartheta}{2}\right)^2 + \eta_\ell^2(p_\ell(\vartheta)) - 4}, \end{aligned} \tag{15}$$

where $p_\ell(\vartheta)$ is the root of the transcendental equation

$$\begin{aligned} &\eta_\ell(p) + \eta_\ell\left(\sqrt{\left(\xi_\ell(p) - 4\cos\frac{\vartheta}{2}\right)^2 + \eta_\ell^2(p) - 4} - \ell\right) = 0,\ p \in (0,\vartheta), \\ &\vartheta \in (\vartheta_\ell^2, 2\pi - \vartheta_\ell^2). \end{aligned}$$

As previously noted, the surface $\tilde{\mathcal{B}}^{-\upsilon}_{\mathcal{TD}}$ crosses $\tilde{\mathcal{B}}^{\upsilon}_{\mathcal{P}}$ only if $\ell \in (0, \ell_J)$. We associate the parameter τ with $\tilde{\mathcal{B}}^{\upsilon}_{\mathcal{P}}$ and τ' with $\tilde{\mathcal{B}}^{-\upsilon}_{\mathcal{TD}}$. Consider the system

$$\begin{aligned} &\bar{z}_{\mathcal{B}^{-\upsilon}_{\mathcal{TD}}}\left(\tau', \vartheta\right) = \bar{z}_{\mathcal{B}^{\upsilon}_{\mathcal{P}}}(\tau,\vartheta),\ \vartheta \in (\vartheta_\ell^1, \vartheta_\ell^2),\ \tau \in \left(0, \pi - \frac{\vartheta}{2}\right), \\ &\tau' \in \left(\frac{\vartheta}{2}, \vartheta\right),\ \ell \in (0, \ell_J). \end{aligned}$$

For $\vartheta \in (\vartheta_\ell^1, \vartheta_\ell^2)$, a unique solution to the system for the given ranges of τ and τ' is

$$\tau = -\frac{\vartheta}{2} + \arccos\left(2\cos\frac{\vartheta}{2} - \frac{\sqrt{(\ell+w_\ell)^2 - \ell^2 + 4}}{2}\right), \quad \tau' = \frac{w_\ell + \vartheta}{2}. \tag{16}$$

The surface $\tilde{\mathcal{B}}^{\upsilon}_{\mathcal{TD}}$ crosses $\tilde{\mathcal{B}}^{-\upsilon}_{\mathcal{TS}}$ only if $\ell \in (\ell_J, +\infty)$. As earlier, we associate parameters τ, τ' with $\tilde{\mathcal{B}}^{-\upsilon}_{\mathcal{TS}}$, $\tilde{\mathcal{B}}^{\upsilon}_{\mathcal{TD}}$, respectively. Consider the system

$$\begin{aligned}
&\bar{z}_{\mathcal{B}^{-\upsilon}_{\mathcal{TS}}}(\tau, \vartheta) = \bar{z}_{\mathcal{B}^{\upsilon}_{\mathcal{TD}}}\left(\tau', 2\pi - \vartheta\right),\\
&\vartheta \in (\vartheta^1_\ell, \vartheta^2_\ell), \quad \tau \in (\vartheta, 2\pi), \quad \tau' \in \left(\pi - \frac{\vartheta}{2}, 2\pi - \vartheta\right), \quad \ell \in (\ell_J, +\infty).
\end{aligned}$$

For $\vartheta \in (\vartheta^1_\ell, \vartheta^2_\ell)$, a unique solution to the system for the given ranges of τ and τ' is given by

$$\tau = \pi - \arcsin \frac{(\ell+\vartheta)^2 - (\ell + q_\ell(\vartheta))^2}{4(\ell+\vartheta)}, \quad \tau' = \pi + \frac{q_\ell(\vartheta) - \vartheta}{2}, \tag{17}$$

where $q_\ell(\vartheta)$ is the root of the transcendental equation

$$\begin{aligned}
&(\ell+\vartheta)^2 - \left(2 + 2\cos\frac{q-\vartheta}{2}\right)^2 - \left(\ell + q + 2\sin\frac{q-\vartheta}{2}\right)^2 = 0,\\
&q \in (0, 2\pi - \vartheta), \quad \vartheta \in (\vartheta^1_\ell, \vartheta^2_\ell), \quad \ell \in (\ell_J, +\infty).
\end{aligned} \tag{18}$$

4.4 Actual Parts of the Barrier

Now, when all conditions of intersection are obtained, we can determine the valid parts of the emanated semipermeable surfaces that constitute the barrier $\mathcal{B}$. First, we describe surface $\mathcal{B}^{\upsilon}_{\mathcal{P}} = \tilde{\mathcal{B}}^{\upsilon}_{\mathcal{P}} \cap \mathcal{B}$. θ-slices of this surface exist for all $\vartheta \in (0, 2\pi)$ (see Figs. 2–3). For all values of ℓ, if $\vartheta \in (0, \vartheta^1_\ell]$, then the intersection is determined by (14). If $\ell \in (0, \ell_J)$, the surface $\tilde{\mathcal{B}}^{\upsilon}_{\mathcal{P}}$ crosses $\tilde{\mathcal{B}}^{-\upsilon}_{\mathcal{TD}}$ and the maximum value of τ is given by (16). Summarizing, we have

$$\mathcal{B}^{\upsilon}_{\mathcal{P}} \stackrel{\text{def}}{=} \left\{\bar{z}_{\mathcal{B}^{\upsilon}_{\mathcal{P}}}(\tau, \vartheta) : \ \vartheta \in (0, 2\pi), \ \tau \in \left(0, \tau^{\max}_{\mathcal{B}_{\mathcal{P}},\ell}(\vartheta)\right)\right\}, \tag{19}$$

where

$$\tau^{\max}_{\mathcal{B}_{\mathcal{P}},\ell}(\vartheta) \stackrel{\text{def}}{=} \begin{cases}
\arccos\left(\cos\frac{\vartheta}{2} - \frac{\sqrt{(\ell+\vartheta)^2 + (\ell - 2\sin\frac{\vartheta}{2})^2}}{2}\right) - \frac{\vartheta}{2}, & \vartheta \in \left(0, \vartheta^1_\ell\right],\\
\arccos\left(2\cos\frac{\vartheta}{2} - \frac{\sqrt{(\ell+w_\ell)^2 - \ell^2 + 4}}{2}\right) - \frac{\vartheta}{2}, & \vartheta \in \left[\vartheta^1_\ell, \vartheta^{21}_\ell\right],\\
\pi - \frac{\vartheta}{2}, & \vartheta \in \left[\vartheta^{21}_\ell, 2\pi\right)
\end{cases}$$

and

$$\vartheta^{21}_\ell \stackrel{\text{def}}{=} \begin{cases}
\vartheta^2_\ell & \ell \in (0, \ell_J],\\
\vartheta^1_\ell, & \ell \in [\ell_J, +\infty).
\end{cases}$$

Next, we describe surface $\mathcal{B}^{\upsilon}_{\mathcal{TS}} = \tilde{\mathcal{B}}^{\upsilon}_{\mathcal{PL}} \cap \mathcal{B}$. θ-slices of this surface exist only for $\vartheta \in (0, \vartheta^1_\ell)$ if $\ell \in (0, \ell_J]$ and for $\vartheta \in (0, \vartheta^2_\ell)$ if $\ell \in (\ell_J, +\infty)$ (see Figs. 2–3). The maximum value of time-to-go τ is determined by τ' of (14) and τ of (17). Thus,

$$\mathcal{B}^{\upsilon}_{\mathcal{TS}} \stackrel{\text{def}}{=} \left\{ \bar{z}_{\mathcal{B}^{\upsilon}_{\mathcal{TS}}}(\tau, \vartheta) : \ \vartheta \in (0, \vartheta^{12}_\ell), \quad \tau \in \left(\vartheta, \tau^{\max}_{\mathcal{B}_{\mathcal{TS}},\ell}(\vartheta) \right) \right\}, \tag{20}$$

where

$$\vartheta^{12}_\ell \stackrel{\text{def}}{=} \begin{cases} \vartheta^1_\ell, & \ell \in (0, \ell_J], \\ \vartheta^2_\ell, & \ell \in [\ell_J, +\infty) \end{cases}$$

and

$$\tau^{\max}_{\mathcal{B}_{\mathcal{TS}},\ell}(\vartheta) \stackrel{\text{def}}{=} \begin{cases} \frac{\vartheta}{2} + \arccos \frac{2 \sin \frac{\vartheta}{2} - \ell}{\ell + \vartheta}, & \vartheta \in (0, \vartheta^1_\ell], \\ \pi - \arcsin \frac{(\ell+\vartheta)^2 - (\ell + q_\ell(\vartheta))^2}{4(\ell+\vartheta)}, & \vartheta \in [\vartheta^1_\ell, \vartheta^{12}_\ell]. \end{cases}$$

Lemma 4.2 $0 < \tau^{\max}_{\mathcal{B}_{\mathcal{TS}},\ell}(\vartheta) < \vartheta + \pi$ *holds for all* $\vartheta \in (0, \vartheta^{12}_\ell]$.

Proof For $\vartheta \in (0, \vartheta^1_\ell]$ (or $\ell \le \ell_J$), this statement is trivial because

$$\tau^{\max}_{\mathcal{B}_{\mathcal{TS}},\ell}(\vartheta) - \vartheta = -\frac{\vartheta}{2} + \arccos \frac{2 \sin \frac{\vartheta}{2} - \ell}{\ell + \vartheta} < \arccos \frac{2 \sin \frac{\vartheta}{2} - \ell}{\ell + \vartheta} \le \pi.$$

For $\vartheta \in (\vartheta^1_\ell, \vartheta^2_\ell]$ (and $\ell > \ell_J$), proving that $q_\ell(\vartheta) < \vartheta$ is sufficient because

$$\tau^{\max}_{\mathcal{B}_{\mathcal{TS}},\ell}(\vartheta) - \vartheta < \tau^{\max}_{\mathcal{B}_{\mathcal{TS}},\ell}(\vartheta) = \pi - \arcsin \frac{(\vartheta - q_\ell(\vartheta))(2\ell + \vartheta + q_\ell(\vartheta))}{4(\ell + \vartheta)} < \pi.$$

Assume the contrary that $q_\ell(\vartheta) \ge \vartheta$. Transform (18) to

$$(\ell + \vartheta)^2 - (\ell + q_\ell(\vartheta))^2 = 8 \left(1 + \cos \frac{q_\ell(\vartheta) - \vartheta}{2} \right) + 4(\ell + q_\ell(\vartheta)) \sin \frac{q_\ell(\vartheta) - \vartheta}{2}.$$

According to (18), the root $q_\ell(\vartheta)$ is less than $2\pi - \vartheta$, implying that $0 \le (q_\ell(\vartheta) - \vartheta)/2 < \pi$. Hence, the left part of the equation is non-positive, whereas the right part is positive. The contradiction completes the proof. □

Further, we will obtain a description of $\mathcal{B}^{\upsilon}_{\mathcal{TD}} = \tilde{\mathcal{B}}^{\upsilon}_{\mathcal{TD}} \cap \mathcal{B}$. θ-slices of this surface exist only for $\vartheta \in (0, 2\pi - \vartheta^2_\ell)$ if $\ell \in (0, \ell_J]$ and for $\vartheta \in (0, 2\pi - \vartheta^1_\ell)$ if $\ell \in [\ell_J, +\infty)$ (see Figs. 2–3). The maximal value of time-to-go τ is determined by τ' of (16), τ' of (17), and τ, τ' of (15). Therefore,

$$\mathcal{B}^{\upsilon}_{\mathcal{TD}} \stackrel{\text{def}}{=} \left\{ \bar{z}_{\mathcal{B}^{\upsilon}_{\mathcal{TD}}}(\tau, \vartheta) : \ \vartheta \in (0, 2\pi - \vartheta^{21}_\ell), \quad \tau \in \left(\frac{\vartheta}{2}, \tau^{\max}_{\mathcal{B}_{\mathcal{TD}},\ell}(\vartheta) \right) \right\}, \tag{21}$$

where

$$\tau^{\max}_{\mathcal{B}_{\mathcal{TD}},\ell}(\vartheta) \stackrel{\text{def}}{=} \begin{cases} \vartheta, & \vartheta \in (0, \vartheta_\ell^{12}], \\ \frac{w_\ell+\vartheta}{2}, & \vartheta \in [\vartheta_\ell^1, \vartheta_\ell^2], \quad \ell \in (0, \ell_J], \\ \frac{p_\ell(\vartheta)+\vartheta}{2}, & \vartheta \in [\vartheta_\ell^2, 2\pi - \vartheta_\ell^2], \\ \frac{q_\ell(2\pi-\vartheta)+\vartheta}{2}, & \vartheta \in [2\pi - \vartheta_\ell^2, 2\pi - \vartheta_\ell^1], \quad \ell \in [\ell_J, +\infty). \end{cases}$$

Finally, we give expressions for $\mathcal{B}^{\upsilon}_{\mathcal{PL}} = \tilde{\mathcal{B}}^{\upsilon}_{\mathcal{PL}} \cap \mathcal{B}$ and $\mathcal{B}^{\upsilon}_{\mathcal{UL}} = \tilde{\mathcal{B}}^{\upsilon}_{\mathcal{UL}} \cap \mathcal{B}$ using the fact that these lines are parts of the boundaries of the corresponding surfaces:

$$\mathcal{B}^{\upsilon}_{\mathcal{PL}} \stackrel{\text{def}}{=} \left\{ \bar{z}_{\mathcal{B}^{\upsilon}_{\mathcal{PL}}}(\vartheta) : \ \vartheta \in (\vartheta_\ell^{21}, 2\pi) \right\}, \ \mathcal{B}^{\upsilon}_{\mathcal{UL}} \stackrel{\text{def}}{=} \left\{ \bar{z}_{\mathcal{B}^{\upsilon}_{\mathcal{UL}}}(\vartheta) : \ \vartheta \in (0, \vartheta_\ell^{12}] \right\}. \tag{22}$$

For completeness, we also provide a parametric description of the barrier dispersal line $\mathcal{B}_{\mathcal{DL}}$. In the description, we use the function

$$\gamma_\theta \stackrel{\text{def}}{=} \begin{cases} -1, & \theta \in (0, \pi], \\ +1, & \theta \in [\pi, 2\pi). \end{cases}$$

For all values of the capture radius ℓ and all θ-slices, the dispersal line is a part of the boundary of $\mathcal{B}^{\upsilon}_{\mathcal{TS}}$ or $\mathcal{B}^{\upsilon}_{\mathcal{TD}}$. Using this fact, we obtain:

$$\mathcal{B}_{\mathcal{DL}} \stackrel{\text{def}}{=} \left\{ z_{\mathcal{B}_{\mathcal{DL}}}(\theta) : \ \theta \in (0, 2\pi) \right\}, \tag{23}$$

where

$$z_{\mathcal{B}_{\mathcal{DL}}}(\theta) \stackrel{\text{def}}{=} \begin{cases} \bar{z}_{\mathcal{B}^{\gamma_\theta}_{\mathcal{TD}}} \left(\tau^{\max}_{\mathcal{B}_{\mathcal{TD}}} \left(\pi - |\pi - \theta| \right), \pi - |\pi - \theta| \right), & \theta \in [\vartheta_\ell^{12}, 2\pi - \vartheta_\ell^{12}], \\ \bar{z}_{\mathcal{B}^{\gamma_\theta}_{\mathcal{TS}}} \left(\tau^{\max}_{\mathcal{B}_{\mathcal{TS}}} \left(\pi - |\pi - \theta| \right), \pi - |\pi - \theta| \right), & \text{otherwise.} \end{cases}$$

Visualization of the surfaces $\mathcal{B}^{\upsilon}_{\mathcal{P}}$, $\mathcal{B}^{\upsilon}_{\mathcal{TS}}$, $\mathcal{B}^{\upsilon}_{\mathcal{TD}}$ and lines $\mathcal{B}^{\upsilon}_{\mathcal{PL}}$, $\mathcal{B}^{\upsilon}_{\mathcal{UL}}$ for the different values of the capture radius ℓ is presented in Fig. 4. These figures show the θ-slices of the 3-dimensional barrier surface $\mathcal{B}$. The colors of the lines and dots correspond to the colored labels with the names of the surfaces and lines. In Fig. 5, we highlight the difference between the small, medium, and large radius cases. If the capture radius is small, then $\mathcal{B}^{+1}_{\mathcal{P}}$ and $\mathcal{B}^{-1}_{\mathcal{TD}}$ have a union part of their boundary. For the large capture radius, the union part is between $\mathcal{B}^{-1}_{\mathcal{TS}}$ and $\mathcal{B}^{+1}_{\mathcal{TD}}$. For the medium capture radius, the union part degenerates into a point where $\mathcal{B}^{+1}_{\mathcal{P}}$, $\mathcal{B}^{-1}_{\mathcal{TD}}$, $\mathcal{B}^{-1}_{\mathcal{TS}}$, and $\mathcal{B}^{+1}_{\mathcal{TD}}$ meet each other.

5 Optimal Feedback Controls on the Barrier

In the previous sections, we obtained parametric descriptions of all the pieces of the barrier with corresponding restrictions on the parameters. Since the values of the

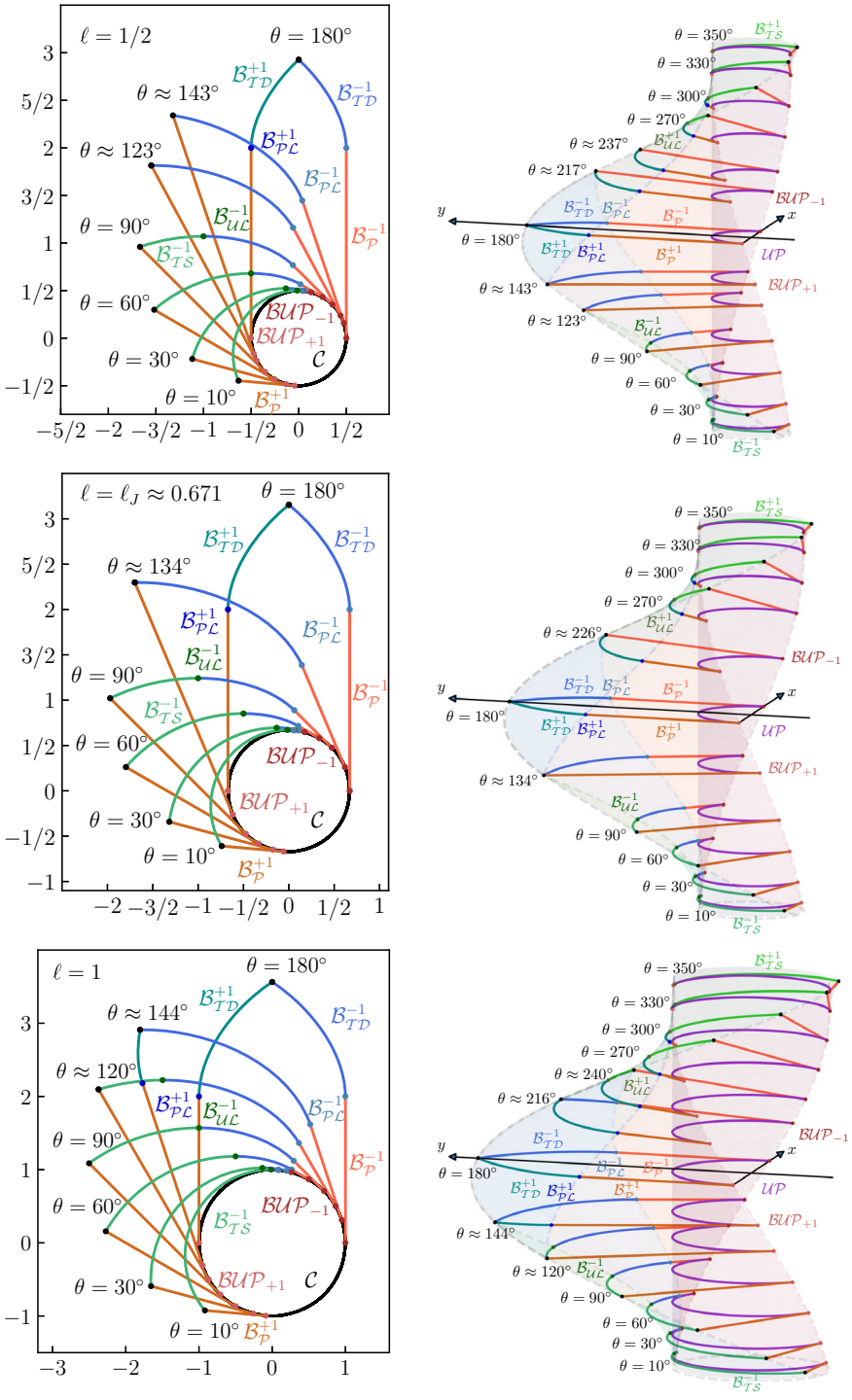

Fig. 4 Barrier cross sections for the small, medium, and large capture radius

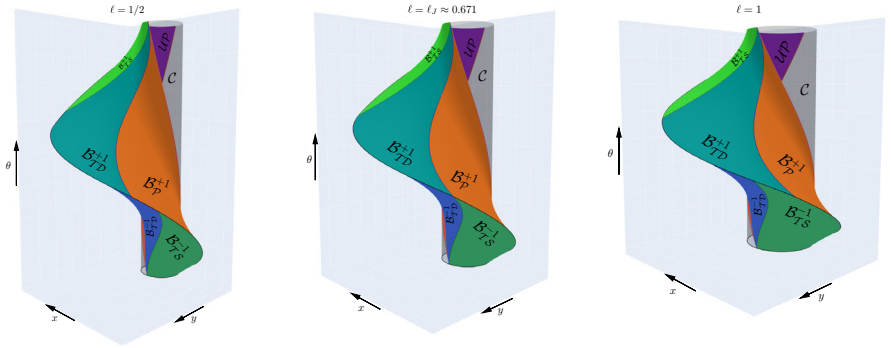

Fig. 5 Difference between the small $\ell \in (0, \ell_J)$ (left figure), medium $\ell = \ell_J$ (middle figure), and large $\ell \in (\ell_J, +\infty)$ (right figure) capture radius cases

optimal controls for both players on each of these pieces are known, by checking which of the pieces the current state belongs to, we can calculate the values of the optimal controls for both players. For the obtained parameterizations (19)–(22), such verification is complicated by the additional calculation of parameters τ and ϑ. Only for the dispersal line $\mathcal{B}_{\mathcal{DL}}$, the parameterization (23) immediately allows checking whether the state $z = \begin{bmatrix} x & y & \theta \end{bmatrix}^\top$ belongs to the dispersal line. In this section, we obtain a parameterization for (19)–(22) using the state vector z.

For GTIC, it will be demonstrated that each piece of the barrier (denoted by $\mathcal{P}$) can be parameterized in the following form:

$$\mathcal{P} = \{z \in \mathcal{F}^{\ell}_{\mathcal{P}} : \ \ell = \ell_{\mathcal{P}}(z)\}. \tag{24}$$

Here, $\mathcal{F}^{\ell}_{\mathcal{P}} \subset \mathbb{R}^2 \times \mathbb{S}$ is the frame set. This corresponds to the restrictions on the parameters τ and ϑ.

To obtain the desired parametric description of $\mathcal{B}^{\upsilon}_{\mathcal{P}}$, we must exclude τ and ϑ from the system of equations

$$\bar{z}_{\mathcal{B}^{\upsilon}_{\mathcal{P}}}(\tau, \vartheta) = z, \quad \vartheta \in (0, 2\pi), \quad \tau \in \left(0, \tau^{\max}_{\mathcal{B}_{\mathcal{P}},\ell}(\vartheta)\right).$$

By applying the transformation $\boldsymbol{R}_{\upsilon}(\vartheta/2)$ we obtain

$$\begin{cases} 2\cos\dfrac{\vartheta}{2} - 2\cos\left(\tau + \dfrac{\vartheta}{2}\right) = -\upsilon x \cos\dfrac{\vartheta}{2} + y \sin\dfrac{\vartheta}{2}, \\ -\ell = \upsilon x \sin\dfrac{\vartheta}{2} + y \sin\dfrac{\vartheta}{2}, \\ (1-\upsilon)\pi + \upsilon\vartheta = \theta, \quad \vartheta \in (0, 2\pi), \quad \tau \in \left(0, \tau^{\max}_{\mathcal{B}_{\mathcal{P}},\ell}(\vartheta)\right). \end{cases}$$

Eliminating ϑ from the second equation, we obtain

$$\ell = -\upsilon\left(x\sin\frac{\theta}{2} + y\cos\frac{\theta}{2}\right) \stackrel{\text{def}}{=} \ell_{\mathcal{B}^{\upsilon}_{\mathcal{P}}}(z).$$

Taking into account that $0 < \tau^{\max}_{\mathcal{B}_{\mathcal{P}},\ell}(\vartheta) < \pi - \vartheta/2$, we transform $\tau \in (0, \tau^{\max}_{\mathcal{B}_{\mathcal{P}},\ell}(\vartheta))$ into

$$-2\cos\frac{\vartheta}{2} < -2\cos\left(\tau + \frac{\vartheta}{2}\right) < -2\cos\left(\tau^{\max}_{\mathcal{B}_{\mathcal{P}},\ell}(\vartheta) + \frac{\vartheta}{2}\right).$$

Substituting ϑ in the first equation and using the obtained inequality, we conclude that

$$\mathcal{F}^{\ell}_{\mathcal{B}^{\upsilon}_{\mathcal{P}}} \stackrel{\text{def}}{=} \left\{z \in \mathbb{R}^2 \times \mathbb{S} :\ 0 < -x\cos\frac{\theta}{2} + y\sin\frac{\theta}{2} < 2\upsilon\left(\cos\frac{\theta}{2} - \cos\left(\tau^{\max}_{\mathcal{B}^{\upsilon}_{\mathcal{P}},\ell}(\theta) + \frac{\upsilon\theta}{2}\right)\right),\ 0 < \theta < 2\pi\right\},$$

where $\tau^{\max}_{\mathcal{B}^{\upsilon}_{\mathcal{P}},\ell}(\theta) = \tau^{\max}_{\mathcal{B}_{\mathcal{P}},\ell}((1-\upsilon)\pi + \upsilon\theta)$.

To obtain the same parametric description for $\mathcal{B}^{\upsilon}_{\mathcal{TS}}$, we must solve the system

$$\bar{z}_{\mathcal{B}^{\upsilon}_{\mathcal{TS}}}(\tau, \vartheta) = z, \quad \vartheta \in (0, \vartheta^{12}_{\ell}), \quad \tau \in \left(\vartheta, \tau^{\max}_{\mathcal{B}_{\mathcal{TS}},\ell}(\vartheta)\right).$$

Expressing $\sin(\tau - \vartheta)$ and $\cos(\tau - \vartheta)$ in the system yields

$$\sin(\tau - \vartheta) = \frac{\upsilon x - 1 + \cos\vartheta}{\ell + \vartheta}, \quad \cos(\tau - \vartheta) = \frac{y + \sin\vartheta}{\ell + \vartheta}.$$

For a fixed $\vartheta \in (0, \vartheta^{12}_{\ell})$, it corresponds to a parametric description of a circle on xy-plane, where τ is a parameter. Using $\tau > \vartheta$ and Lemma 4.2 we obtain

$$\sin(\tau - \vartheta) > 0, \quad \cos(\tau - \vartheta) > \cos(\tau^{\max}_{\mathcal{B}_{\mathcal{TS}},\ell}(\vartheta) - \vartheta).$$

Expressing ϑ and substituting in these inequalities, we obtain the frame

$$\mathcal{F}^{\ell}_{\mathcal{B}^{\upsilon}_{\mathcal{TS}}} \stackrel{\text{def}}{=} \{z \in \mathbb{R}^2 \times \mathbb{S} :\ 0 < (1+\upsilon)\pi - \upsilon\theta < \vartheta^{12}_{\ell},\ 1 - \cos\theta < \upsilon x, \\ (\ell + (1+\upsilon)\pi - \upsilon\theta)\cos(\tau^{\max}_{\mathcal{B}^{\upsilon}_{\mathcal{TS}},\ell}(\theta) + \upsilon\theta) < y - \upsilon\sin\theta\},$$

where $\tau^{\max}_{\mathcal{B}^{\upsilon}_{\mathcal{TS}},\ell}(\theta) = \tau^{\max}_{\mathcal{B}_{\mathcal{TS}},\ell}((1+\upsilon)\pi - \upsilon\theta)$. Eliminating τ from the circle parameterization and expressing ℓ, we have

$$\ell = -(1+\upsilon)\pi + \upsilon\theta + \sqrt{(\upsilon x - 1 + \cos\theta)^2 + (y - \upsilon\sin\theta)^2} \stackrel{\text{def}}{=} \ell_{\mathcal{B}^{\upsilon}_{\mathcal{TS}}}(z).$$

To obtain the parametric description for $\mathcal{B}^{\upsilon}_{\mathcal{TD}}$ we have to exclude τ and ϑ from the system of equations

$$\bar{z}_{\mathcal{B}^{\upsilon}_{\mathcal{TD}}}(\tau,\vartheta)=z,\quad \vartheta\in(0,2\pi-\vartheta^{21}_{\ell}),\quad \tau\in\left(\vartheta/2,\tau^{\max}_{\mathcal{B}_{\mathcal{TD}},\ell}(\vartheta)\right).$$

Expressing $\sin(\tau-\vartheta)$ and $\cos(\tau-\vartheta)$ from the system gives

$$\sin(\tau-\vartheta)=\frac{(\upsilon x+1+\cos\vartheta)(\ell+2\tau-\vartheta)-2(y+\sin\vartheta)}{(\ell+2\tau-\vartheta)^2+4},$$
$$\cos(\tau-\vartheta)=\frac{2(\upsilon x+1+\cos\vartheta)+(y+\sin\vartheta)(\ell+2\tau-\vartheta)}{(\ell+2\tau-\vartheta)^2+4}.$$

The sum of squares of these values and inequality $\ell+2\tau-\vartheta>0$ give

$$\ell+2\tau-\vartheta=\sqrt{(\upsilon x+1+\cos\vartheta)^2+(y+\sin\vartheta)^2-4}. \tag{25}$$

Since $\tau-\vartheta\in(-\vartheta/2,\tau^{\max}_{\mathcal{B}_{\mathcal{TD}},\ell}(\vartheta)-\vartheta)\subset(-\pi,0)$, $\sin(\tau-\vartheta)$ must be negative. Hence, we can invert $\cos(\tau-\vartheta)$ to

$$\tau-\vartheta=-\arccos\frac{2(\upsilon x+1+\cos\vartheta)+(y+\sin\vartheta)(\ell+2\tau-\vartheta)}{(\ell+2\tau-\vartheta)^2+4}. \tag{26}$$

Combining (25) and (26), and using $\vartheta=(1+\upsilon)\pi-\upsilon\theta$ we obtain

$$\begin{aligned}\ell=&\sqrt{(\upsilon x+1+\cos\theta)^2+(y-\upsilon\sin\theta)^2-4}-(1+\upsilon)\pi+\upsilon\theta\\&+2\arccos\left(\frac{2(\upsilon x+1+\cos\theta)}{(\upsilon x+1+\cos\theta)^2+(y-\upsilon\sin\theta)^2}\right.\\&\left.+\frac{(y-\upsilon\sin\theta)\sqrt{(\upsilon x+1+\cos\theta)^2+(y-\upsilon\sin\theta)^2-4}}{(\upsilon x+1+\cos\theta)^2+(y-\upsilon\sin\theta)^2}\right)\overset{\text{def}}{=}\ell_{\mathcal{B}^{\upsilon}_{\mathcal{TD}}}(z).\end{aligned}$$

Given the above, the frame is described by

$$\begin{aligned}&\mathcal{F}^{\ell}_{\mathcal{B}^{\upsilon}_{\mathcal{TD}}}\overset{\text{def}}{=}\{z\in\mathbb{R}^2\times\mathbb{S}:\ 0<(1+\upsilon)\pi-\upsilon\theta<2\pi-\vartheta^{21}_{\ell},\\&0<-\ell+\sqrt{(\upsilon x+1+\cos\theta)^2+(y-\upsilon\sin\theta)^2-4}\\&\quad<2\tau^{\max}_{\mathcal{B}^{\upsilon}_{\mathcal{TD}},\ell}(\theta)-(1+\upsilon)\pi+\upsilon\theta,\\&(\upsilon x+1+\cos\theta)\sqrt{(\upsilon x+1+\cos\theta)^2+(y-\upsilon\sin\theta)^2-4}<2(y-\upsilon\sin\theta)\},\end{aligned}$$

where $\tau^{\max}_{\mathcal{B}^{\upsilon}_{\mathcal{TD}},\ell}(\theta)=\tau^{\max}_{\mathcal{B}_{\mathcal{TD}},\ell}((1+\upsilon)\pi-\upsilon\theta)$.

The parametric descriptions (22) of $\mathcal{B}^{\upsilon}_{\mathcal{PL}}$ and $\mathcal{B}^{\upsilon}_{\mathcal{UL}}$ contain only one parameter ϑ which can be expressed through θ in both cases. Hence,

$$\mathcal{B}^{\upsilon}_{\mathcal{PL}} = \{z \in \mathbb{R}^2 \times \mathbb{S} : \bar{z}_{\mathcal{B}^{\upsilon}_{\mathcal{PL}}}((1-\upsilon)\pi + \upsilon\theta) = z,\ \vartheta_{\ell}^{21} < (1-\upsilon)\pi + \upsilon\theta < 2\pi\},$$
$$\mathcal{B}^{\upsilon}_{\mathcal{UL}} = \{z \in \mathbb{R}^2 \times \mathbb{S} : \bar{z}_{\mathcal{B}^{\upsilon}_{\mathcal{UL}}}((1+\upsilon)\pi - \upsilon\theta) = z,\ 0 < (1+\upsilon)\pi - \upsilon\theta \le \vartheta_{\ell}^{12}\}.$$

Proposition 5.1 *The optimal feedback controls on the barrier for the pursuer and evader in the GTIC are given by*

$$u^*(z) = \begin{cases} 0, & z \in \mathcal{B}^{-1}_{\mathcal{UL}} \cup \mathcal{B}^{+1}_{\mathcal{UL}}; \\ +1, & z \in \mathcal{B}^{-1}_{\mathcal{P}} \cup \mathcal{B}^{-1}_{\mathcal{PL}} \cup \mathcal{B}^{+1}_{\mathcal{TS}} \cup \mathcal{B}^{-1}_{\mathcal{TD}} \cup \mathcal{BUP}_{-1} \cup \mathcal{B}_{\mathcal{D}}\mathcal{L}; \\ -1, & z \in \mathcal{B}^{+1}_{\mathcal{P}} \cup \mathcal{B}^{+1}_{\mathcal{PL}} \cup \mathcal{B}^{-1}_{\mathcal{TS}} \cup \mathcal{B}^{+1}_{\mathcal{TD}} \cup \mathcal{BUP}_{+1} \cup \mathcal{B}_{\mathcal{D}}\mathcal{L}; \\ \operatorname{sgn} x, & z \in \mathcal{BUP}_0, \end{cases}$$

$$v^*(z) = \begin{cases} +1, & z \in \mathcal{B}^{+1}_{\mathcal{P}} \cup \mathcal{B}^{+1}_{\mathcal{PL}} \cup \mathcal{B}^{+1}_{\mathcal{TS}} \cup \mathcal{B}^{+1}_{\mathcal{TD}} \cup \mathcal{B}^{+1}_{\mathcal{UL}} \cup \mathcal{BUP}_{+1} \cup \mathcal{B}_{\mathcal{D}}\mathcal{L}; \\ -1, & z \in \mathcal{B}^{-1}_{\mathcal{P}} \cup \mathcal{B}^{-1}_{\mathcal{PL}} \cup \mathcal{B}^{-1}_{\mathcal{TS}} \cup \mathcal{B}^{-1}_{\mathcal{TD}} \cup \mathcal{B}^{-1}_{\mathcal{UL}} \cup \mathcal{BUP}_{-1} \cup \mathcal{B}_{\mathcal{D}}\mathcal{L}; \\ \operatorname{sgn} x, & z \in \mathcal{BUP}_0. \end{cases}$$

Proposition 5.1 provides optimal feedback control on the barrier. All parts of the barrier were explicitly described using analytical expressions in terms of the state vector. Thus, the problem of calculating the feedback control on the barrier is completely solved. Note that the process of trimming the excess parts of the barrier, as described in the previous section, provided an analytical description of the ranges of parameter changes. This analytical description is used in the description of the frame sets $\mathcal{F}^{\ell}_{\mathcal{P}}$, which in turn participates in the explicit description of the barrier pieces.

Direct calculations with floating points will almost always miss the barrier because the barrier is a two-dimensional manifold in a three-dimensional space. A natural method to avoid this problem is to check for belonging to the layer

$$\mathcal{P}' = \left\{ z \in \mathcal{F}^{\ell_{\mathcal{P}}(z)}_{\mathcal{P}} : \ \ell \le \ell_{\mathcal{P}}(z) \le \ell(1+\delta) \right\}$$

adjacent to the piece of barrier surface $\mathcal{P}$ given by (24). Here, $\delta \in \mathbb{R}^+$ denotes the relative layer width. If the calculations are precise, the evader can guarantee evasion with the minimal approaching distance $\ell(1+\delta)$.

6 Conclusions

In this study, we have derived a complete analytical description of the barrier for the GTIC. The obtained description is provided for all possible values of capture radius. Analysis of the variation in the barrier geometry with a variation in the capture radius showed that there are differences between the shape of the barrier for small and large values of the capture radius. These differences indicate that the analytical conditions for cutting off redundant parts of semipermeable surfaces that constitute the barrier have different forms.

Considering the classification of possible forms of the barrier depending on the capture radius, it is no longer necessary to use the trial-and-error method to construct the barrier, as has been done in other approaches when analyzing the barrier of the GTIC. In addition, we obtained a parametric description of the barrier in terms of the state vector. Such a description makes it possible to synthesize feedback optimal control that does not require the elimination of additional parameters by numerical methods. Thus, the resulting control can be calculated directly from the state vector.

For the collision avoidance problem, the expression obtained for the evader's optimal feedback control on the barrier can be made resistant to the rounding error of the state vector. To achieve this, instead of calculating the control for the barrier surface, we must calculate the control for the state belonging to the layer whose boundary is the barrier itself. Indicator of belonging to such a layer can also be established using explicit analytical calculations. This makes evasive control more attractive for practical implementations.

One possible avenue for further research is to investigate the barrier of the GTC using the same methods.

Acknowledgements The research was supported by RSF (project No. 23-19-00134).

Data Availability All data generated or analyzed during this study are included in this published article.

Compliance with ethical standards

Conflict of interest The authors have no conflicts of interest to declare.

References

1. Baron, S., Chu, K.C., Ho, Y.C., Kleinman, D.L.: A new approach to aerial combat games. Tech. Rep. NASA-CR-1626, Harvard University (1970)
2. Bera, R., Makkapati, V.R., Kothari, M.: A comprehensive differential game theoretic solution to a game of two cars. J. Optim. Theory Appl. **174**(3), 818–836 (2017). https://doi.org/10.1007/s10957-017-1134-z
3. Borówko, P., Rzymowski, W.: On the game of two cars. J. Optim. Theory Appl. **44**(3), 381–396 (1984). https://doi.org/10.1007/bf00935458
4. Breakwell, J.V., Merz, A.W.: Minimum required capture radius in a coplanar model of the aerial combat problem. AIAA J. **15**(8), 1089–1094 (1977). https://doi.org/10.2514/3.7399
5. Ciletti, M.D., Merz, A.W.: Collision avoidance maneuvers for ships. Navigation **23**(2), 128–135 (1976). https://doi.org/10.1002/j.2161-4296.1976.tb00731.x
6. Cockayne, E.: Plane pursuit with curvature constraints. SIAM J. Appl. Math. **15**(6), 1511–1516 (1967). https://doi.org/10.1137/0115133
7. Farber, N., Shinar, J.: Approximate solution of singularly perturbed nonlinear pursuit-evasion games. J. Optim. Theory Appl. **32**(1), 39–73 (1980). https://doi.org/10.1007/BF00934842
8. Greenfeld, I.: A differential game of surveillance evasion of two identical cars. J. Optim. Theory Appl. **52**(1), 53–79 (1987). https://doi.org/10.1007/BF00938464
9. Isaacs, R.: Differential Games: A Mathematical Theory with Applications to Warfare and Pursuit, Control and Optimization. John Wiley and Sons Inc, New York (1965)
10. Kostsov, A.V., Simakova, E.N.: Differential game an conventional ways to solve the pursuit problem. Autom. Remote Control **49**(11), 1423–1432 (1988)
11. Kwik, K.H.: Calculation of ship collision avoidance manoeuvres: a simplified approach. Ocean Eng. **16**(5), 475–491 (1989). https://doi.org/10.1016/0029-8018(89)90048-6

12. Lewin, J.: Differential Games: Theory and Methods for Solving Game Problems with Singular Surfaces. Springer Science & Business Media, Berlin (2012). https://doi.org/10.1007/978-1-4471-2065-0
13. Maurer, H., Tarnopolskaya, T., Fulton, N.: Singular controls in optimal collision avoidance for participants with unequal linear speeds. ANZIAM J. **53**, 1–18 (2011). https://doi.org/10.21914/anziamj.v53i0.5098
14. Maurer, H., Tarnopolskaya, T., Fulton, N.: Optimal bang-bang and singular controls in collision avoidance for participants with unequal linear speeds. In: 2012 IEEE 51st IEEE Conference on Decision and cCntrol (CDC) 2012. IEEE, pp. 7697–7702 2012). https://doi.org/10.1109/CDC.2012.6426792
15. Maurer, H., Tarnopolskaya, T., Fulton, N.: Computation of bang-bang and singular controls in collision avoidance. J. Ind. Manag. Optim. **10**(2), 443–460 (2014). https://doi.org/10.3934/jimo.2014.10.443
16. Meier, L.: A new technique for solving pursuit-evasion differential games. IEEE Trans. Autom. Control **14**(4), 352–359 (1969). https://doi.org/10.1109/TAC.1969.1099226
17. Merz, A.W.: The game of two identical cars. J. Optim. Theory Appl. **9**(5), 324–343 (1972). https://doi.org/10.1007/BF00932932
18. Merz, A.W.: Optimal evasive maneuvers in maritime collision avoidance. Navigation **20**(2), 144–152 (1973). https://doi.org/10.1002/j.2161-4296.1973.tb01163.x
19. Merz, A.W.: The homicidal chauffeur. AIAA J. **12**(3), 259–260 (1974). https://doi.org/10.2514/3.49215
20. Merz, A.W., Karmarkar, J.S.: Collision avoidance systems and optimal turn manoeuvres. J. Navig. **29**(2), 160–174 (1976). https://doi.org/10.1017/s0373463300030150
21. Miloh, T.: Determination of critical maneuvers for collision avoidance using the theory of differential games. Tech. Rep. 319, Institut für Schiffbau der Uni Hamburg (1974)
22. Miloh, T.: The game of two elliptical ships. Optim. Control Appl. Methods **4**(1), 13–29 (1983). https://doi.org/10.1002/oca.4660040103
23. Miloh, T., Pachter, M.: Ship collision-avoidance and pursuit-evasion differential games with speed-loss in a turn. Comput. Math. Appl. **18**(1), 77–100 (1989). https://doi.org/10.1016/0898-1221(89)90126-0
24. Miloh, T., Sharma, S.D.: Maritime collision avoidance as a differential game. Schiffstechnik **24**(116), 69–88 (1977)
25. Mitchell, I.: Games of two identical vehicles. Tech. Rep. SUDAAR #740, Stanford University (2001)
26. Olsder, G.J., Walter, J.L.: A differential game approach to collision avoidance of ships. In: Stoer, J. (ed.) Optimization Techniques Part 1, pp. 264–271. Springer, Berlin (1978)
27. Pachter, M., Coates, S.: The classical homicidal chauffeur game. Dyn. Games Appl. **9**(3), 800–850 (2019). https://doi.org/10.1007/s13235-018-0264-8
28. Pachter, M., Getz, W.M.: The geometry of the barrier in the game of two cars. Optim. Control Appl. Methods **1**(2), 103–118 (1980). https://doi.org/10.1002/oca.4660010202
29. Pachter, M., Miloh, T.: The geometric approach to the construction of the barrier surface in differential games. Comput. Math. Appl. **13**(1–3), 47–67 (1987). https://doi.org/10.1016/0898-1221(87)90093-9
30. Rublein, G.T.: On pursuit with curvature constraints. SIAM J. Control. Optim. **10**(1), 37–39 (1972). https://doi.org/10.1137/0310003
31. Sharma, S.D.: On ship maneuverability and collision avoidance. Tech. Rep. 352, Institut für Schiffbau der Uni Hamburg (1977)
32. Simakova, E.N.: Differential pursuit game. Autom. Remote Control **28**(2), 173–181 (1967)
33. Simakova, E.N.: Problem of pursuit and evasion. Autom. Remote Control **31**(8), 1205–1211 (1970)
34. Simakova, E.N.: On optimal strategies in games of pursuit with limited maneuverability. Autom. Remote Control **44**(10), 1307–1315 (1983)
35. Simakova, E.N.: On bellman functions in optimization of dynamic systems under uncertainty. Autom. Remote Control **47**(2), 47–51 (1986)
36. Tarnopolskaya, T., Fulton, N.: Optimal cooperative collision avoidance strategy for coplanar encounter: Merz's solution revisited. J. Optim. Theory Appl. **140**(2), 355–375 (2009). https://doi.org/10.1007/s10957-008-9452-9
37. Tarnopolskaya, T., Fulton, N.: Synthesis of optimal control for cooperative collision avoidance for aircraft (ships) with unequal turn capabilities. J. Optim. Theory Appl. **144**(2), 367–390 (2010). https://doi.org/10.1007/s10957-009-9597-1
38. Tarnopolskaya, T., Fulton, N.L.: Non-unique optimal collision avoidance strategies for coplanar encounter of participants with unequal turn capabilities. IAENG Int. J. Appl. Math. **40**(4), 289–296 (2010)

39. Tarnopolskaya, T., Fulton, N.L.: Synthesis of optimal control for cooperative collision avoidance in a close proximity encounter: special cases. IFAC Proc. **44**(1), 9775–9781 (2011). https://doi.org/10.3182/20110828-6-IT-1002.00325
40. Vincent, T.L., Cliff, E.M., Grantham, W.J., Peng, W.Y.: A problem of collision avoidance. Tech. Rep. NASA-CR-129988, University of Arizona (1972)
41. Vincent, T.L., Cliff, E.M., Grantham, W.J., Peng, W.Y.: Some aspects of collision avoidance. AIAA J. **12**(1), 3–4 (1974). https://doi.org/10.2514/3.49141
42. Vincent, T.L., Sticht, D.J., Peng, W.Y.: Aircraft missile avoidance. Oper. Res. **24**(3), 420–437 (1976). https://doi.org/10.1287/opre.24.3.420
43. Weintraub, I.E., Pachter, M., Garcia, E.: An introduction to pursuit-evasion differential games. In: 2020 American Control Conference (ACC), pp. 1049–1066 (2020). https://doi.org/10.23919/ACC45564.2020.9147205